[16] R.F. Chen, Removal of fatty acids from serum albumin by charcoal treatment, J. Biol. Chem. 242 (1967) 173–181.
[17] E. Meucci, A. Mordente, G.E. Martorana, Metal-catalyzed oxidation of human serum albumin: conformational and functional changes, J. Biol. Chem. 266 (1991) 4692–4699.
[18] I. Climent, L. Tsai, R.L. Levine, Derivatization of gamma-glutamyl semialdehyde residues in oxidized proteins by fluoresceinamine, Anal. Biochem. 182 (1989) 226–232.
[19] D.J. Hnatowich, W.W. Latne, R.L. Childs, The preparation and labeling of DTPA-coupled albumin, Int. J. Appl. Isot. 33 (1982) 327–332.
[20] F. Staud, M. Nishikawa, K. Morimoto, Y. Takakura, M. Hashida, Disposition of radioactivity after injection of liver-targeted proteins labeled with ^{111}In or ^{125}I. Effect of labeling on distribution and excretion of radioactivity in rats, J. Pharm. Sci. 88 (1999) 577–585.
[21] J.R. Duncan, M.J. Welch, Intracellular metabolism of indium 111-DTPA-labeled receptor targeted proteins, J. Nucl. Med. 34 (1993) 1728–1738.
[22] K. Yamaoka, Y. Tanigawara, T. Nakagawa, T. Uno, A pharmacokinetic analysis program (multi) for microcomputer, J. Pharmacobio-dyn. 4 (1981) 879–885.
[23] T. Mukai, Y. Arano, K. Nishida, H. Sasaki, H. Saji, J. Nakamura, In-vivo evaluation of indium-111-diethylenetri-aminepentaacetic acid labelling for determining the sites and rates of protein catabolism in mice, J. Pharm. Pharmacol. 51 (1999) 15–20.
[24] P.G. Pande, R.V. Nellore, H.R. Bhagat, Optimization and validation of analytical conditions for bovine serum albumin using capillary electrophoresis, Anal. Biochem. 204 (1992) 103–106.
[25] M. Anraku, K. Yamasaki, T. Maruyama, U. Kragh-Hansen, M. Otagiri, Effect of oxidative stress on the structure and function of human serum albumin, Pharm. Res. 18 (2001) 632–639.
[26] S. Sugio, A. Kashima, S. Mochizuki, M. Noda, K. Kobayashi, Crystal structure of human serum albumin at 2.5 A resolution, Protein Eng. 12 (1999) 439–446.
[27] K. Nakajou, H. Watanabe, U. Kragh-Hansen, T. Maruyama, M. Otagiri, The effect of glycation on the structure, function and biological fate of human serum albumin as revealed by recombinant mutants, Biochim. Biophys. Acta 1623 (2003) 88–97.
[28] H.L. Segal, D.M. Rothstein, J.R. Winkler, A correlation between turnover rates and lipophilic affinities of soluble rat liver proteins, Biochem. Biophys. Res. Commun. 73 (1976) 79–84.
[29] A.A. Bhattacharya, T. Grüne, S. Curry, Crystallographic analysis reveals common modes of binding of medium and long-chain fatty acids to human serum albumin, J. Mol. Biol. 303 (2000) 721–732.
[30] H. Watanabe, U. Kragh-Hansen, S. Tanase, K. Nakajou, M. Mitarai, Y. Iwao, T. Maruyama, M. Otagiri, Conformational stability and warfarin-binding properties of human serum albumin studied by recombinant mutants, Biochem. J. 357 (2001) 269–274.
[31] N. Ahmed, D. Dobler, M. Dean, P.J. Thornalley, Peptide mapping identifies hotspot site of modification in human serum albumin by methylglyoxal involved in ligand binding and esterase activity, J. Biol. Chem. 280 (2005) 5724–5732.
[32] B. Smedsrød, J. Melkko, N. Araki, H. Sano, S. Horiuchi, Advanced glycation end products are eliminated by scavenger-receptor-mediated endocytosis in hepatic sinusoidal, Kupffer and endothelial cells, Biochem. J. 322 (1997) 567–573.
[33] K. Matsumoto, H. Sano, R. Nagai, H. Suzuki, T. Kodama, M. Yoshida, S. Ueda, B. Smedsrød, S. Horiuchi, Endocytic uptake of advanced glycation end products by mouse liver sinusoidal endothelial cells is mediated by a scavenger receptor distinct from the macrophage scavenger receptor class A, Biochem. J. 352 (2000) 233–240.
[34] T. Kodama, M. Freeman, L. Rohrer, J. Zabrecky, P. Matsudaira, M. Krieger, Type I macrophage scavenger receptor contains alpha-helical and collagen-like coiled coils, Nature 343 (1990) 531–535.
[35] J.F. Nagelkerke, K.P. Barto, T.J.C. van Berkel, In vivo and in vitro uptake and degradation of acetylated low density lipoprotein by rat liver endothelial, Kupffer and parenchymal cells, J. Biol. Chem. 258 (1983) 12221–12227.
[36] L. Malerod, K. Juvet, T. Gjoen, T. Berg, The expression of scavenger receptor class B, type I (SR-BI) and caveolin-1 in parenchymal and nonparenchymal liver cells, Cell Tissue Res. 307 (2002) 173–180.
[37] M.J. Duryee, T.L. Freeman, M.S. Willis, C.D. Hunter, B.C. Hamilton, H. Suzuki, D.J. Tuma, L.W. Klassen, G.M. Thiele, Scavenger receptors on sinusoidal liver endothelial cells are involved in the uptake of aldehyde-modified proteins, Mol. Pharmacol. 68 (2005) 1423–1430.
[38] H. Adachi, M. Tsujimoto, H. Arai, K. Inoue, Expression cloning of a novel scavenger receptor from human endothelial cells, J. Biol. Chem. 272 (1997) 31217–31220.
[39] B. Hansen, P. Longati, K. Elvevold, G.I. Nedredal, K. Schledzewski, R. Olsen, M. Falkowski, J. Kzhyshkowska, F. Carlsson, S. Johansson, B. Smedsrød, S. Goerdt, S. Johansson, P. McCourt, Stabilin-1 and stabilin-2 are both directed into the early endocytic pathway in hepatic sinusoidal endothelium via interactions with clathrin/AP-2, independent of ligand binding, Exp. Cell Res. 303 (2005) 160–173.
[40] Y. Tamura, H. Adachi, J. Osuga, K. Ohashi, N. Yahagi, M. Sekiya, H. Okazaki, S. Tomita, Y. Iizuka, H. Shimano, R. Nagai, S. Kimura, M. Tsujimoto, S. Ishibashi, FEEL-1 and FEEL-2 are endocytic receptors for advanced glycation end products, J. Biol. Chem. 278 (2003) 12613–12617.
[41] J.E. Schnitzerand, J. Bravo, High affinity binding, endocytosis, and degradation of conformationally modified albumins: potential role of gp30 and gp18 as novel scavenger receptors, J. Biol. Chem. 268 (1993) 7562–7570.
[42] R. Bito, S. Hino, A. Baba, M. Tanaka, H. Watabe, H. Kawabata, The degradation of oxidative stress-induced denatured albumin in rat liver endothelial cells, Am. J. Physiol.: Cell Physiol. 289 (2005) C531–C542.
[43] K. Nakajou, S. Horiuchi, M. Sakai, K. Hirata, M. Tanaka, M. Takeya, T. Kai, M. Otagiri, CD36 is not involved in scavenger receptor-mediated endocytic uptake of glycolaldehyde- and methylglyoxal-modified proteins by liver endothelial cells, J. Biochem. (Tokyo) 137 (2005) 607–616.

Drug Metab. Pharmacokinet. 21 (2): 140–146 (2006).

Regular Article

The Structural and Pharmacokinetic Properties of Oxidized Human Serum Albumin, Advanced Oxidation Protein Products (AOPP)

Yasunori IWAO[1], Makoto ANRAKU[1], Mikako HIRAIKE[1], Keiichi KAWAI[2], Keisuke NAKAJOU[1], Toshiya KAI[3], Ayaka SUENAGA[1] and Masaki OTAGIRI[1,*]

[1]*Department of Biopharmaceutics, Graduate School of Pharmaceutical Sciences, Kumamoto University, Kumamoto, Japan*
[2]*School of Health Sciences, Faculty of Medicine, Kanazawa University, Ishikawa, Japan*
[3]*Pharmaceutical Research Center, Nipro Corporation, Kusatsu, Shiga, Japan*

Full text of this paper is available at http://www.jstage.jst.go.jp/browse/dmpk

Summary: To determine the pharmacokinetic properties of advanced oxidation protein products (AOPP), we prepared oxidized human serum albumin (oxi-HSA) using chloramine-T (a hypochlorite analogue) *in vitro*. The AOPP and dityrosine content of oxi-HSA (AOPP content, $244.3 \pm 12.3\ \mu M$; dityrosine content, 0.7 ± 0.11 nmol of dityrosine/mg protein) were similar to those of uremic patients. In structural analysis, the increases in AOPP and dityrosine content of HSA induced slight decreases in its α-helical content. In pharmacokinetic analysis, oxi-HSA left the circulation rapidly, and organ distribution of oxi-HSA 30 min after intravenous injection was 51% for the liver, 23% for the spleen, and 9% for the kidney, suggesting that the liver and spleen were the main routes of plasma clearance of oxi-HSA. The liver and spleen uptake clearance of oxi-HSA were significantly greater than those of normal HSA (CLliver, 5058 ± 341.6 vs $24 \pm 4.2\ \mu L/hr$ [$p < 0.01$]; CLspleen, 2118 ± 322.1 vs $32 \pm 2.7\ \mu L/hr$ [$p < 0.01$]). However, uptake by other organs was not significantly affected by oxidation. These results suggest that the liver and spleen play important roles in elimination of AOPP.

Key words: human serum albumin; structural change; advanced oxidation protein products; pharmacokinetics

Introduction

Recent evidence indicates that oxidative stress plays an important role in the pathogenesis of chronic renal failure (CRF).[1] Oxidative stress is defined as increased production of reactive oxygen species (ROS) due to an imbalance of oxidant/antioxidant systems. Activated phagocytes are a major source of ROS, and play a fundamental role in host defense.[2] Neutrophils contain the heme enzyme myeloperoxidase (MPO), which catalyzes the reaction of chloride ion with hydrogen peroxide (H_2O_2), to generate the large amounts of hypochlorous acid (HOCl) produced by neutrophils.[3] HOCl-modified proteins have been detected in atherosclerotic lesions[4] and plasma from glomerular nephritis patients.[5] To estimate the degree of oxidant-mediated protein damage in plasma of CRF patients, researchers have assayed levels of advanced oxidation protein products (AOPP) in CRF plasma. Witko-Sarsat *et al.* showed that *in vivo* levels of AOPP strongly correlate with creatinine clearance, indicating that AOPP are excellent markers of progression of CRF.[6] HOCl-treated HSA and *in vivo*-generated AOPP can trigger oxidative bursts in neutrophils and monocytes *in vitro*, indicating that they both can act as true inflammatory mediators.[7] Results of *in vitro* studies of mechanisms of AOPP production indicate that HOCl-treated HSA can trigger an oxidative burst.[7] However, the mechanisms by which AOPP are degraded and eliminated from circulating blood remain unclear.

Recently, there have been reports of several types of receptors that bind to modified albumin, including SR-A (human scavenger receptor class A, which binds LDL)[8,9] and CD36 (scavenger receptor class B family).[10,11] Despite such important findings, it remains unclear whether physiologically oxidized HSA (oxi-

Received; October 14, 2005, Accepted; November 25, 2005
**To whom correspondence should be addressed*: Prof. Masaki OTAGIRI, Ph.D., *Department of Biopharmaceutics, Graduate School of Pharmaceutical Sciences, Kumamoto University, 5-1 Oe-honmachi, Kumamoto 862-0973, Japan. Tel. +81-96-371-4150, Fax. +81-96-362-7690, E-mail: otagirim@gpo.kumamoto-u.ac.jp*

HSA) containing AOPP behaves in the same way as other modified albumins.

In the present study, using normal HSA and chloramine-T-treated HSA (oxi-HSA), we examined the mechanisms by which AOPP are degraded and eliminated from circulating blood.

Material and Methods

Materials and animals: Chloramine-T (CT) was purchased from Nacalai Tesque, Inc. (Kyoto, Japan). The fluorescence probe 1, 1-bis-4-anilino-naphthalene-5,5-sulfonic acid (bis-ANS) was purchased from Sigma (St Louis, MO, USA). $^{111}InCl_3$ (74 MBq/mL in 0.02 N HCl) was donated by Nihon Medi-Physics (Takarazuka, Japan). All chemicals used were of the highest grade commercially available, and all solutions were prepared using deionized, distilled water. Male ddY mice (24–26 g) were purchased from the Shizuoka Agricultural Cooperative Association for Laboratory Animals (Shizuoka, Japan). Animals were maintained under conventional housing conditions. All animal experiments were conducted in accordance with the principles and procedures outlined in the National Institute of Health Guide for the Care and Use of Laboratory Animals.

Preparation of oxi-HSA: HSA (300 μM) was incubated for 1 h at 37°C in an oxygen-saturated solution containing 100 mM CT in phosphate buffer (pH 8.0). After incubation, the oxidation reaction was stopped by extensive dialysis of the solution against water. As a negative control, albumin was incubated in buffer alone. The oxi-HSA and negative control HSA were stored at −20°C until used.

Western blot analysis: Oxi-HSA was detected by performing Western blot analysis. The antibodies used were an anti-HSA primary antibody raised in a rabbit and an anti-rabbit secondary antibody conjugated to horseradish peroxidase.

Determination of AOPP and dityrosine content: AOPP content of oxi-HSA was determined using a previously reported semi-automated method.[6] Dityrosine content was assayed by measuring fluorescence after the sample was diluted to 2 μM. Fluorescence emission spectra of dityrosine were recorded at 410 nm after excitation at 325 nm, using a spectrofluorometer (FP-6200 Jasco) as described previously.[12]

Amino acid analysis: The amino acid composition of oxi-HSA was quantified by performing amino acid analysis after acid hydrolysis with 6 M HCl for 24 h at 110°C, using an amino acid analyzer (L-8500A, Hitachi, Tokyo, Japan) as described previously.[13]

Structural properties of oxi-HSA: CD spectra were obtained using a JASCO J-720 spectropolarimeter (JASCO, Tokyo, Japan) at 25°C. The effective hydrophobicity of oxi-HSA was estimated using the fluorescent characteristics of bis-ANS (10 μM) at 25°C. Each compound was excited at 394 nm, and fluorescence spectra were recorded on a Jasco FP-770 fluorescence spectrometer (Tokyo, Japan).

***In Vivo* Experiments:** All proteins were radiolabeled with ^{111}In using the bifunctional chelating reagent DTPA anhydride, according to the method of Hnatowich *et al.*.[14,15] Mice received tail vein injections of ^{111}In-labeled proteins in saline, at a dose of 1 mg/kg, and were housed in metabolic cages to allow the collection of urine samples. At appropriate intervals after the injection, blood was collected from the vena cava under ether anesthesia, and plasma was obtained by centrifugation. The liver, kidney, spleen, lung, heart and muscle were excised, rinsed with saline and weighed. The radioactivity of each sample was measured using a well-type NaI scintillation counter (ARC-500, Aloka, Tokyo). Pharmacokinetic analyses were performed as follows. The plasma ^{111}In radioactivity concentrations were normalized with respect to the percentage of the dose per mL, and were analyzed using the nonlinear least-square program MULTI.[16] Tissue distribution was evaluated using the organs uptake clearance method (CLorgans), as described previously.[17]

Cellular assays: Endocytic uptake was determined as described previously.[18,27] RAW 264.7 cells were seeded in each well of a 24-well culture plate in 1.0 mL RPMI 1640 medium, containing 10% FCS, 100 U/mL penicillin, and 100 μg/mL streptomycin, and cultured for 12 hr to subconfluence. The cells were washed with 1.0 mL PBS and replaced with Dulbecco's modified Eagle's medium containing 3% BSA, 100 U/mL penicillin, and 100 μg/mL streptomycin (medium A). The cells in each well were incubated at 37°C for 6 hr in 0.5 mL medium A with various concentrations of ^{125}I-control- or oxi-HSA in the presence (non-specific) or absence (total) of 50-fold unlabeled each ligands. At the indicated time, 0.375 mL of the culture medium was taken from each well and mixed with 0.15 mL 40% trichloroacetic acid (TCA) in a vortex mixer. We added 0.1 mL of 0.7 mol/L $AgNO_3$ to this solution, which was followed by centrifugation. The resulting supernatant (0.25 mL) was used to determine TCA-soluble radioactivity, which was taken as an index of cellular degradation, since proteins are endocytosed by the cells and delivered to lysosomes where they are degraded and excreted into the culture medium in a TCA-soluble form. Then, each well was washed three times with 1.0 mL ice-cold PBS. The cells were lysed with 1.0 mL of 0.1 N NaOH for 1 hr at 37°C to determine the cell-associated radioactivity. Specific cell-association or degradation were determined by subtracting non-specific from total.

Statistics: Statistical analyses were performed using

Student's t-test.

Results

Western blot analysis of oxi-HSA: After exposure to CT, protein aggregation or cross-linking was clearly indicated by the presence of a smear in the high molecular weight range. The high-molecular-weight fragments were recognized by the anti-HSA antibody (**Fig. 1**). These results suggest that treatment of HSA with CT causes aggregation and cross-linking due to oxidation (oxi-HSA).

The characteristics of oxi-HSA: The AOPP content of oxi-HSA was significantly greater than that of control-HSA (244.3 ± 12.3 vs 10.3 ± 6.3 μM; $p<0.01$; **Table 1**). Dityrosine content of oxi-HSA was also significantly greater than that of control-HSA (0.7 ± 0.11 vs 0.32 ± 0.13 nmol dityrosine per mg protein; $p<0.01$). These characteristics of oxi-HSA are similar to those of proteins in uremic plasma (**Table 1**). The results of amino acid analysis indicate that oxidation of HSA induced significant changes in its content of certain amino acid residues including tyrosine and basic amino acids (**Table 2**).

Structural properties of oxi-HSA: To obtain information about protein structure, CD measurements were performed in the far-UV regions (**Fig. 2A**). The molar ellipticity of oxi-HSA was significantly less than that of control-HSA in the far-UV CD spectrum. The effects of oxidation on the structural properties were examined using the fluorescence probe bis-ANS. The spectra indicate that oxidation of HSA causes a decrease in its accessible hydrophobic areas (**Fig. 2B**). These results suggest that the structure of HSA is significantly changed by oxidation.

Pharmacokinetic properties of oxi-HSA: **Figure 3A** shows the time courses for radioactivity of ^{111}In-labeled preparations of oxi-HSA. Oxi-HSA had a shorter half-life than control-HSA. To determine the reasons for the decreased plasma half-life of oxi-HSA, we examined organ uptake. Liver, spleen and kidney uptake of oxi-HSA increased with time, and were all much greater than those of control-HSA (**Fig. 3B-D, Table 3**). Uptake by other organs was not significantly affected by oxidation (data not shown).

Discussion

Although *in vivo* studies indicate that the constant plasma half-life of radioisotope-labeled native albumin is 2 to 2.5 days in rats,[19] modified albumin has been

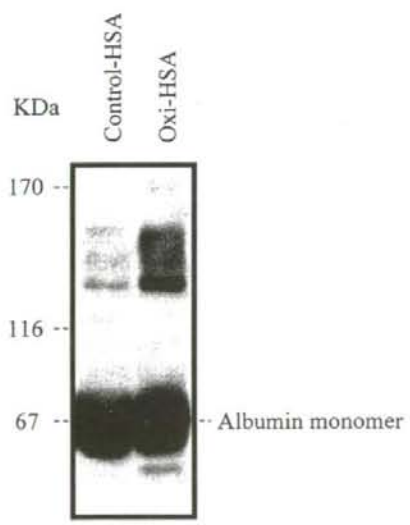

Fig. 1. Western blot analysis of control-HSA and oxi-HSA.

Table 2. Changes in amino acids composition of oxi-HSA.

Amino acids	Literature value	Control-HSA (n = 3)	Oxi-HSA (n = 3)
Thr	28	22.5 ± 0.3	22.4 ± 0.4
Ser	24	24.5 ± 0.2	24.6 ± 0.3
Gly	12	12.0 ± 0.3	12.8 ± 0.3
Ala	62	62.0 ± 0.4	62.0 ± 0.1
Val	41	38.6 ± 0.2	39.4 ± 0.4
Met	6	3.2 ± 0.1	2.14 ± 0.2
Ile	8	7.7 ± 0.5	7.8 ± 0.1
Leu	61	61.3 ± 0.4	61.8 ± 0.1
Tyr	18	16.0 ± 0.3	6.7 ± 0.4*
Lys	59	53.0 ± 0.1	26.9 ± 0.4*
His	16	15.1 ± 0.4	14.5 ± 0.4
Arg	24	23.9 ± 0.4	18.6 ± 0.3*

*Significantly different ($P<0.01$) from control-HSA. Data are mean ± SD.

Table 1. AOPP and dityrosine content of HSA treated with chloramine T.

	Control-HSA	Oxi-HSA	Normal subjects	HD patients
AOPP (μM)	10.3 ± 6.3	244.3 ± 12.3*	33.9 ± 3.4[6]	267.5 ± 16.5[6]
Dityrosine (nmol/mg protein)	0.32 ± 0.13	0.7 ± 0.11*	0.36 ± 0.05[6]	1.03 ± 0.12[6]

*Significantly different ($P<0.01$) from control-HSA. Data are mean ± SD.
[6]Ref. 6.

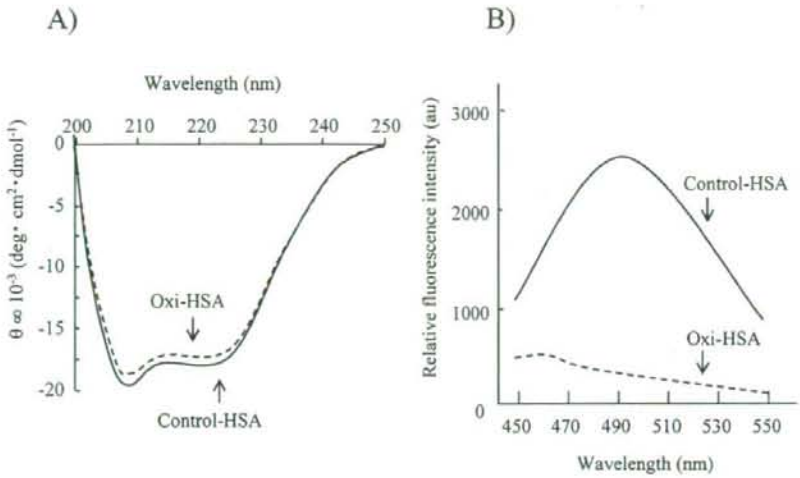

Fig. 2. Far-UV CD spectra (A) and relative fluorescence intensity of hydrophobicity using bis-ANS (B) of control-HSA (—) and oxi-HSA (···). Data are mean ± SD.

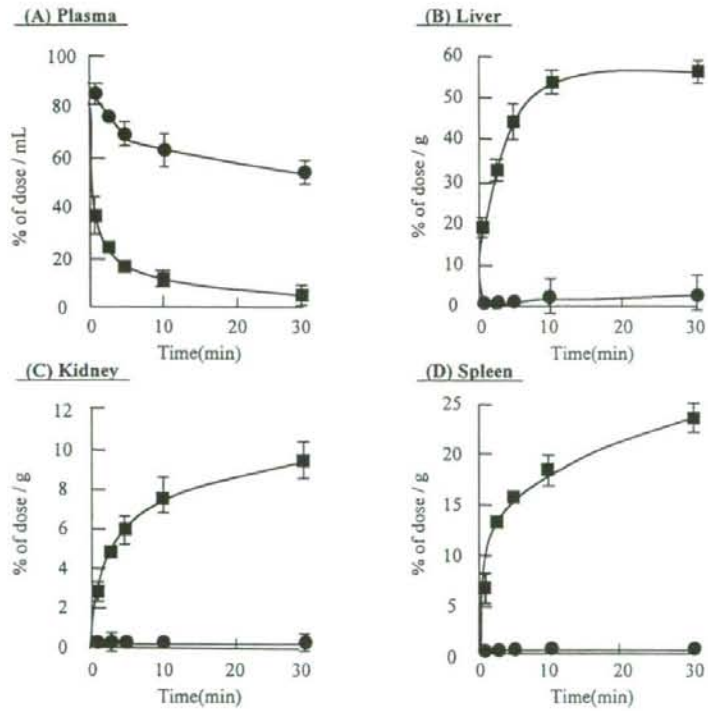

Fig. 3. Plasma and organ levels of ^{111}In-labeled control-HSA (●) and oxi-HSA (■) after i.v. administration to mice. Data are mean ± SD.

shown to have an extremely short half-life in circulating blood.[20] As one of reasons for the formation of modified albumin *in vivo*, free radical species have been found to induce conformational changes, degradation and aggregation of proteins in several diseases.[21] In uremic patients, AOPP are produced by HOCl-modified albumin cross-linking *in vivo*. Further, AOPP can act as mediators of oxidative stress, and they have

been implicated in the immune dysregulation associated with chronic uremia.[6,7] However, the mechanisms by which AOPP is degraded or eliminated from circulating blood remain unclear. Therefore, in the present study, we used CT-treated HSA (oxi-HSA) to examine the mechanisms involved in elimination of AOPP.

The AOPP and dityrosine content of oxi-HSA were similar to those of proteins from uremic plasma (**Table 1**). In the Western blot analysis, oxi-HSA was mostly present in the form of multimolecular aggregates, probably resulting from dityrosine cross-linking and/or disulfide bridges (**Fig. 1**). Further, the amino acid analysis indicates that oxidation of HSA induced significant modification of tyrosine and basic amino acid residues such as lysine and arginine (**Table 2**). These results suggest that the modifications of those amino acid residues are responsible for the conformational changes observed in HSA (**Fig. 2**).

The pharmacokinetic analysis consistently showed that oxi-HSA left the circulation rapidly. The organ distribution 30 min after the intravenous injection was 51% for the liver, 23% for the spleen, and 9% for the kidney, suggesting that the liver was the main route for plasma clearance (**Fig. 3**). Since many of the scavenger receptors are expressed in sinusoidal endothelial cells and Kupffer cells in the liver,[22,23] plural scavenger receptors may be responsible for the hepatic uptake of oxi-HSA. In general, most scavenger receptors can bind a variety of polyanionic ligands, including negatively charged albumins.[24,25] In some diseases including diabetes, AGE-albumins have well known as major negatively charged proteins in plasma. AGE-albumins are nonenzymatically glycosylated proteins that accumulate in vascular tissue with aging and accumulate at accelerated rates in diabetic patients. Schmidt *et al.*[22] reported that AGE-albumins plasma clearance in mice was rapid, with 70% of the injected dose removed from the circulation within 5 min. In their study, liver was also the main route for plasma clearance of AGE-albumin. Their data are very similar to the present findings for oxi-HSA. Interestingly, oxi-HSA has a negatively charged molecule due to the modifications of basic amino acid residues in structural analysis (**Table 2**). Further, oxi-HSA has known to contain a structural motif of AGE-proteins as a result of oxidation.[6,7] Therefore, oxi-HSA are possible to be distributed for liver nonparenchymal cells (endothelial and Kupffer cells) as same as those of AGE-albumins. However, the evidence for scavenger receptor involved in the elimination of modified albumin, including AGE-albumin and oxi-HSA, on liver nonparenchymal cells has been rarely found.[26,27] Unfortunately, we were also unable to clarify the receptor responsible for hepatic uptake in this study, but we should examine the elimination mechanism of oxi-HSA by using cell line highly expressed scavenger receptors in the future.

On the other hands, scavenger receptors are expressed not only on liver nonparenchymal cells but also various macrophages. Given the fact that the organ distribution of oxi-HSA was 23% for the spleen, oxi-HSA may be also taken up by macrophage of spleen via scavenger receptor-mediated endocytosis. Macrophage has known to express highly SR-A, one of the scavenger receptor.[8] To examine the relationship between oxi-HSA and SR-A in macrophage, we used the macrophage-derived cell line RAW 264.7. Significant amounts of ^{125}I-oxi-HSA were associated with these cells and underwent endocytic degradation within the cells, whereas no such findings were observed for control-HSA (**Fig. 4**). Thus, SR-A may be involved in the spleen clearance of oxi-HSA.

Table 3. Uptake clearance of control- and oxi-HSA labeled with ^{111}In after i.v. administration to mice.

(μL/hr)	Liver	Kidney	Spleen
Control-HSA	24 ± 4.2	48 ± 5.3	32 ± 2.7
Oxi-HSA	5058 ± 341.6*	1188 ± 208.2*	2118 ± 322.1*

*Significantly different ($P < 0.01$) from control-HSA.
Data are mean ± SD.

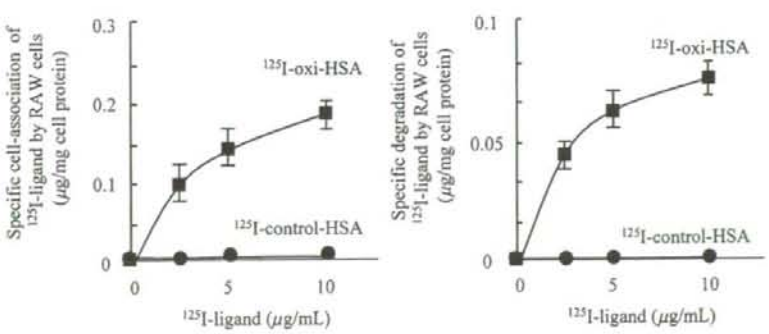

Fig. 4. Endocytic uptake of ^{125}I-labeled control-HSA (●) or oxi-HSA (■) by RAW 264.7 cells. Data are mean ± SD.

In summary, the kinetics of chloramine-T-treated HSA (oxi-HSA) are similar to those of AOPP in uremic patients. Oxi-HSA left the circulation rapidly and accumulated in the liver, spleen and kidney. The liver and spleen appear to play particularly important roles in elimination of AOPP.

References

1) Sies, H.: Oxidative stress: oxidants and antioxidants. *Exp. Physiol.*, **82**: 291–295 (1997).
2) Odajima, J. and Onishi, M.: Biological significance and mechanisms of reactions and events mediated by myeloperoxidase in the xenobiotic metabolism and disposition pathways of leucocytes. *Med. Sci. Res.*, **26**: 291–298 (1998).
3) Kettle, A. J. and Winterbourn, C. C.: Myeloperoxidase: a key regulator of neutrophil oxidant production. *Redox. Rep.*, **3**: 3–15 (1997).
4) Brasen, J. H., Hakkinen, T., Malle, E., Beisiegel, U. and Yla-Herttuala, S.: Patterns of oxidized epitopes, but not NF-kappa B expression, change during atherogenesis in WHHL rabbits. *Atherosclerosis.*, **166**: 13–21 (2003).
5) Grone, H. J., Grone, E. F. and Malle, E.: Immunohistochemical detection of hypochlorite-modified proteins in glomeruli of human membranous glomerulonephritis. *Lab. Invest.*, **82**: 5–14 (2002).
6) Witko-Sarsat, V., Frielander, M., Capeillere-Blandin, C., Nguyen-Khoa, T., Nguyen, A., Zingraff, T. J., Jungers, P. and Descamps-Latscha, B.: Advanced oxidation protein products as a novel marker of oxidative stress in uremia. *Kidney Int.*, **49**: 1304–1313 (1996).
7) Witko-Sarsat, V., Frielander, M., Nguyen-Khoa, T., Capeillere-Blandin, C., Nguyen, A. T., Canteloup, S., Dayer, J. M., Jungers, P., Drueke, T. and Descamps-Latscha, B.: Advanced oxidation protein products as novel mediators of inflammation and monocyte activation in chronic renal failure. *J. Immunol.*, **161**: 2524–2532 (1998).
8) Kodama, T., Freeman, M., Rohrer, L., Zabrecky, J., Matsudaira, P. and Krieger, M.: Type I macrophage scavenger receptor contains alpha-helical and collagen-like coiled coils. *Nature.*, **343**: 531–535 (1990).
9) Neeper, M., Schmidt, A. M., Brett, J., Yan, S. D., Wang, F., Pan, Y. C., Elliston, K., Stern, D. and Shaw, A.: Cloning and expression of a cell surface receptor for advanced glycosylation end products of proteins. *J. Biol. Chem.*, **267**: 14998–15004 (1992).
10) Kuniyasu, A., Ohgami, N., Hayashi, S., Miyazaki, A., Horiuchi, S. and Nakayama, H.: CD36-mediated endocytic uptake of advanced glycation end products (AGE) in mouse 3T3-L1 and human subcutaneous adipocytes. *FEBS Lett.*, **537**: 85–90 (2003).
11) Ohgami, N., Nagai, R., Ikemoto, M., Arai, H., Kuniyasu, A., Horiuchi, S. and Nakayama H.: CD36, a member of the class b scavenger receptor family, as a receptor for advanced glycation end products. *J. Biol. Chem.*, **276**: 3195–3202 (2001).
12) Heinecke, J. W., Li, W. and Daehnke, H. J.: Dityrosine, a specific marker of oxidation, is synthesized by the myeloperoxidase-hydrogen peroxide system of human neutrophils and macrophages. *J. Biol. Chem.*, **268**: 4069–4077 (1993).
13) Nagai, R., Araki, T., Hayashi, C. M., Hayase, F. and Horiuchi, S.: Identification of N epsilon-(carboxyethyl)lysine, one of the methylglyoxal-derived AGE structures, in glucose-modified protein: mechanism for protein modification by reactive aldehydes. *J. Chromatogr. B. Analyt. Technol. Biomed. Life. Sci.*, **5**: 75–84 (2003).
14) Hnatowich, D. J., Latne, W. W. and Childs, R. L.: The preparation and labeling of DTPA-coupled albumin. *Int. J. Appl. Isot.*, **33**: 327–332 (1982).
15) Staud, F., Nishikawa, M., Morimoto, K., Takakura, Y. and Hashida, M.: Disposition of radioactivity after injection of liver-targeted proteins labeled with ^{111}In or ^{125}I. Effect of labeling on distribution and excretion of radioactivity in rats. *J. Pharm. Sci.*, **88**: 577–585 (1999).
16) Yamaoka, K., Tanigawara, Y., Nakagawa, T. and Uno, T.: A pharmacokinetic analysis program (multi) for microcomputer. *J. Pharmacobiodyn.*, **4**: 879–885 (1981).
17) Anraku, M., Kragh-Hansen, U., Kawai, K., Maruyama, T., Yamasaki, Y., Takakura, Y. and Otagiri, M.: Validation of the chloramine-T induced oxidation of human serum albumin as a model for oxidative damage *in vivo*. *Pharm. Res.*, **20**: 684–692 (2003).
18) Nagai, R., Matsumoto, K., Ling, X., Suzuki, H., Araki, T. and Horiuchi, S.: Glycolaldehyde, a reactive intermediate for advanced glycation end products, plays an important role in the generation of an active ligand for the macrophage scavenger receptor. *Diabetes.*, **49**: 1714–1723 (2000).
19) Peters, T. Jr.: All About Albumin: Biochemistry, Genetics, and Medical Applications. San Diego, Academic Press, Inc., 1996.
20) Mego, J. L.: Role of thiols, pH and cathepsin D in the lysosomal catabolism of serum albumin. *Biochem. J.*, **218**: 775–783 (1984).
21) Davies, K. J. and Delsignore, M. E.: Protein damage and degradation by oxygen radicals. III. modification of secondary and tertiary structure. *J. Biol. Chem.*, **262**: 9908–9913 (1987).
22) Schmidt, A. M., Hasu, M. and Popov, D.: Receptor for advanced glycation end products (AGEs) has a central role in vessel wall interactions and gene activation in response to circulating AGE proteins. *Proc. Natl. Acad. Sci. U S A.*, **91**: 8807–8811 (1994).
23) Smedsrød, B., Melkko, J., Araki, N., Sano, H. and Horiuchi, S.: Advanced glycation end products are eliminated by scavenger-receptor-mediated endocytosis in hepatic sinusoidal Kupffer and endothelial cells. *Biochem. J.*, **322**: 567–573 (1997).
24) Horiuchi, S., Takata, K., Maeda, H. and Morino Y.: Scavenger function of sinusoidal liver cells. Acetylated low-density lipoprotein is endocytosed *via* a route distinct from formaldehyde-treated serum albumin. *J. Biol. Chem.*, **260**: 53–56 (1985).
25) Vlassara, H., Brownlee, M. and Cerami, A.: Novel macrophage receptor for glucose-modified proteins is distinct from previously described scavenger receptors.

J. Exp. Med., **164**: 1301–1309 (1986).
26) Matsumoto, K., Sano, H., Nagai, R., Suzuki, H., Kodama, T., Yoshida, M., Ueda, S., Smedsrød, B. and Horiuchi, S.: Endocytic uptake of advanced glycation end products by mouse liver sinusoidal endothelial cells is mediated by a scavenger receptor distinct from the macrophage scavenger receptor class *A*. *Biochem. J.*, **352**: 233–240 (2000).
27) Nakajou, K., Horiuchi, S., Sakai, M., Hirata, K., Tanaka, M., Takeya, M., Kai, T. and Otagiri M.: CD36 is not involved in scavenger receptor-mediated endocytic uptake of glycolaldehyde- and methylglyoxal-modified proteins by liver endothelial cells. *J. Biochem (Tokyo).*, **137**: 607–616 (2005).

Pharmaceutical Research, Vol. 23, No. 5, May 2006 (© 2006)
DOI: 10.1007/s11095-006-9933-1

Research Paper

Recombinant Human Serum Albumin Dimer has High Blood Circulation Activity and Low Vascular Permeability in Comparison with Native Human Serum Albumin

Sadaharu Matsushita,[1] Victor Tuan Giam Chuang,[1,2] Masanori Kanazawa,[1] Sumio Tanase,[3] Keiichi Kawai,[4] Toru Maruyama,[1] Ayaka Suenaga,[1] and Masaki Otagiri[1,5]

Received September 8, 2005; accepted January 12, 2006

Purpose. Human serum albumin (HSA) is used clinically as an important plasma expander. Albumin infusion is not recommended for critically ill patients with hypovolemia, burns, or hypoalbuminemia because of the increased leakage of albumin into the extravascular spaces, thereby worsening edema. In the present study, we attempted to overcome this problem by producing a recombinant HSA (rHSA) dimer with decreased vascular permeability and an increased half-life.
Methods. Two molecules of rHSA were genetically fused to produce a recombinant albumin dimer molecule. The pharmacokinetics and biodistribution of the recombinant proteins were evaluated in normal rats and carrageenin-induced paw edema mouse model.
Results. The conformational properties of this rHSA dimer were similar to those for the native HSA (the HSA monomer), as evidenced by the Western blot and spectroscopic studies. The biological half-life and area under the plasma concentration–time curve of the rHSA dimer were approximately 1.5 times greater than those of the monomer. Dimerization has also caused a significant decrease in the total body clearance and distribution volume at the steady state of the native HSA. rHSA dimer accumulated to a lesser extent in the liver, skin, muscle, and fat, as compared with the native HSA. Up to 96 h, the vascular permeability of the rHSA dimer was less than that of the native HSA in paw edema mouse models. A prolonged plasma half-life of the rHSA dimer was also observed in the edema model rats.
Conclusions. rHSA dimer has a high retention rate in circulating blood and a lower vascular permeability than that of the native HSA.

KEY WORDS: biodistribution; human serum albumin; pharmacokinetic analysis; recombinant human serum albumin dimer; vascular permeability.

INTRODUCTION

Human serum albumin (HSA), the most abundant protein in plasma, is responsible for 80% of the colloid osmotic pressure of plasma (25–33 mmHg). Because of this, it is mainly used clinically to maintain colloid oncotic pressure and to increase the circulating plasma volume (1). HSA product was developed for the treatment of shock where HSA Fraction V, USP, served as an attractive agent for the correction of hypovolemia, burns, and various diseases that result in albumin loss. In spite of the many theoretical benefits of albumin infusion in critically ill patients, there has been little evidence to support its widespread clinical use. For many years, albumin infusion was believed to improve vital prognosis. Recently, a meta-analysis that included 24 studies involving 1419 patients published by Cochran Injuries Group Albumin Reviewers suggested that the administration of albumin-containing fluids resulted to a 1.68 times increase in the relative risk of death when compared to a crystalloid solution (2). In contrast, no difference in mortality was reported in a large-scale clinical trial in Australia and New Zealand, in which 4% albumin was compared to 0.9% sodium chloride for intravascular fluid resuscitation in patients in intensive care units (ICUs) (3).

Reviews published on the parenteral use of albumin and the consensus of several conferences recommended that the administration of HSA can be justified for acute circulatory

[1] Department of Biopharmaceutics, Graduate School of Pharmaceutical Sciences, Kumamoto University, 5-1 Oe-honmachi, Kumamoto 862-0973, Japan.
[2] Department of Pharmacy, Faculty of Allied Health Sciences, Universiti Kebangsaan Malaysia, Jalan Raja Muda Abdul Aziz, 50300 Kuala Lumpur Malaysia.
[3] Department of Analytical Biochemistry, School of Health Sciences, Kumamoto University, 4-24-1 Kuhonji, Kumamoto 862-0976, Japan.
[4] School of Health Sciences, Faculty of Medicine, Kanazawa University, 5-11-80 Kodatsuno, Kanazawa 920-1192, Japan.
[5] To whom correspondence should be addressed. (e-mail: otagirim@gpo.kumamoto-u.ac.jp

ABBREVIATIONS: AUC, area under the plasma concentration–time curve; CL_{tot}, total body clearance; HSA, human serum albumin; rHSA, recombinant HAS; Vd_{ss}, distribution volume of the steady state; %ID, percentage of injected dose.

problems caused by hypovolemia, but it is seldom warranted and is used merely to increase albumin concentrations in cases of hypoalbuminemia (4). Only shock due to recent blood loss is an indication of the use of parenteral albumin, because the incidence of shock to acute-phase or hyperallergic reactions is accompanied by increased albumin flux to the extravascular compartment and adding to the albumin pool in this case would only expand this compartment and bring on edema (5–7). The lung is particularly susceptible to albumin overloading, and albumin administration for respiratory distress has been a matter of debate because of the possibility that pulmonary edema may result (8,9). Cardiac failure is another hazard of an overzealous increase in circulatory volume (10).

It is well known that capillary protein permeability is increased in many pathological and physiological conditions. For instance, the rate of protein extravasation may increase up to 100 times the normal rate in burn injury. Under such conditions, the albumin molecules administered as a plasma expander are transported to organs and cause a further accumulation of fluids, hence worsening the disease. The frequent administration of albumin infusion to maintain the desired blood concentration, as well as the oncotic pressure, inevitably leads to the poor retention of albumin infused during the disease state. Although albumin receptors have been reported to mediate the transport of albumin across the cellular membrane, the mechanism of leakage during inflammation may involve a different route of extravasation since cytokines are known to loosen tight junctions (11).

In other words, if a form of albumin that possesses good blood retention and low extravasation properties could be developed, the frequency of administration could be decreased and further accumulation of fluids in tissues could be prevented. Hence, increasing the molecular size of albumin to stop leakage to extravascular spaces may be a potential solution in making albumin a superior candidate as a volume replacement therapeutic agent. This type of albumin would not only be superior for clinical use but would also be useful pharmacoeconomically.

In addition, since albumin is typically harvested using conventional techniques involving the fractionation of plasma obtained from blood donors, possible viral/prion contaminants contained in the preparation impose risk to users. As a solution to this problem, the development of recombinant technology in producing therapeutic proteins such as HSA has been promoted. In this study, we genetically fused two molecules of HSA and used *Pichia pastoris* to express the recombinant HSA (rHSA) dimer protein. The pharmacokinetic and pharmacological properties of the rHSA dimer were then evaluated.

MATERIALS AND METHODS

Materials

Native HSA was donated by the Chemo-Sera-Therapeutic Research Institute (Kumamoto, Japan) and defatted by means of a charcoal treatment as described by Chen (12). A chimeric plasmid (pJDB-ADH-L10-HAS-A) having cDNA for the mature form of HSA along with an L10 leader sequence was a gift from Tonen Co. (Tokyo, Japan). The restriction enzymes *Eco*RI, *Xho*I, *Ava*I, *Bam*HI, and *Sal*I and *E. coli* JM109 were obtained from Takara Shuzo Co., Ltd. (Kyoto, Japan). KOD-Plus-DNA polymerase was obtained from Toyobo Co., Ltd. (Osaka, Japan). The restriction enzyme *Pci*I was obtained from New England Biolabs (Beverly, MA, USA). A DNA sequence kit was obtained from Perkin-Elmer Applied Biosystems (Foster City, CA, USA). The *Pichia* Expression Kit and the restriction enzyme *Nco*I were purchased from Invitrogen Corp. (Carlsbad, CA, USA). [^{125}I] Iodine-125 was purchased from Amersham Biosciences Corp. (Piscataway, NJ, USA). [^{111}In] Indium chloride was supplied by Nihon Medi-Physics (Takarazuka, Japan). Trichloroacetic acid (TCA) was purchased from Nakalai Tesque (Kyoto, Japan). λ-Carrageenin was purchased from Sigma (St. Louis, MO, USA). Other chemicals used were obtained from commercial suppliers.

Synthesis, Purification, and Structure Analysis of rHSA Dimer

An rHSA dimer in which two HSA molecules are linked with an amino acid linker $(GGGGS)_2$ was designed. The rHSA dimer expression vector was constructed through the four-piece ligation of the following: (1) pPIC9K vector was digested with *Bam*HI and *Eco*RI; (2) the fragment derived from the digestion of pPIC9K with *Bam*HI and *Xho*I restriction sites was amplified by PCR; (3) the PCR product on the 5′ side of the rHSA dimer, amplified using HSA cDNA as the template, was digested with *Xho*I and *Ava*I (HSAcDNA-1); (4) the PCR product on the 3′ side of rHSA dimer, which was amplified using HSA cDNA as the template, was digested with *Ava*I and *Eco*RI (HSAcDNA-2). These four DNA fragments were separated from the cleavage products by agarose gel electrophoresis and purified.

Construction of the expression vector of the rHSA dimer was achieved by a four-piece ligation (Fig. 1). The resulting vector was transformed into *E. coli* JM109 and amplified. The sequence of the rHSA dimer in the resulting vector was confirmed by verifying the sequence of gel extract cDNA fragments of the resulting vector digested by *Pci*I or *Nco*I. The resulting vector was introduced into the yeast *P. pastoris* (strain GS115), and the rHSA dimer was expressed and purified. The purified rHSA dimer was confirmed by N-terminal amino acid sequences analysis, sodium dodecyl sulfate polyacrylamide gel electrophoresis (SDS-PAGE), and Western blot analysis. The structure of the rHSA dimer was estimated from fluorescence and circular dichroism (CD) spectral data (13).

Transformation, Expression, and Purification of the rHSA Dimer

Construction of the expression vector of the rHSA dimer was made by a four-piece ligation (Fig. 1). The resulting vector was transformed into *E. coli* JM109 and amplified. The sequence of the rHSA dimer in the resulting vector was confirmed on gel extracts of the cDNA fragments of the resulting vector digested by *Pci*I or *Nco*I. The resulting vector was linearized with *Sal*I and introduced into the yeast

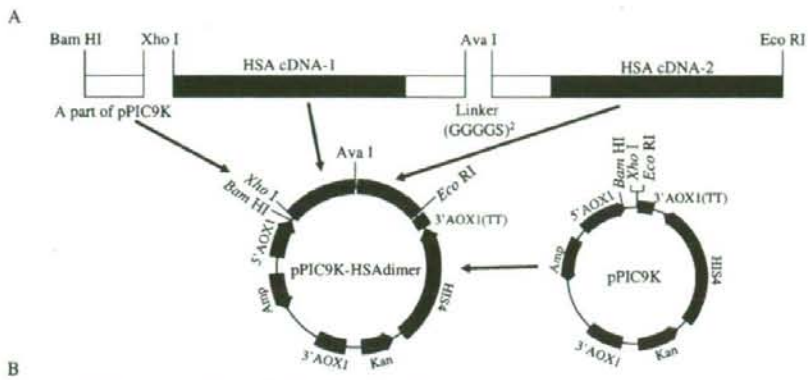

B

A part of pPIC9K, sense: 5'-CGA AGG ATC CAA ACG ATG AG-3'
Bam HI

antisense: 5'-CTT TTC TCG AGA GAT ACC CCT TCT TC-3'
Xho I

HSA cDNA-1, sense: 5'-GGT ACC CTC GAG AAA AGA GAT GCA CAC AAG AGT GAG GTT GC-3'
Xho I

antisense: 5'-CAG CTG **CC CGA GCC ACC ACC ACC** TAA GCC TAA GGC AGC TTG ACT TGC-3'
Ava I

HSA cDNA-2, sense: 5'-GTT AAC **C TCG GGC GGT GGC GGA AGT** GAT GCA CAC AAG AGT GAG GTT GC-3'
Ava I

antisense: 5'-CAC GTG GAA TTC TTA TAA GCC TAA GGC AGC TTG ACT TGC-3'
Eco RI

Fig. 1. Schematic of the pPIC9K expression vector containing the rHSA dimer gene (A) and the sequence of the primers used in the construction of the rHSA dimer (B). The restriction site sequences are underlined. The linker regions are in boldface.

P. pastoris (strain GS115) by electroporation using a GENE-PULSER II (Bio-Rad, Hercules, CA, USA) according to the manufacturer's instruction from Invitrogen. His^+ colonies were subcultured in yeast protein dextrose (YPD) and plated on YPD agars containing 0.25–3 mg/mL to select for multicopy recombinants. A 1-mL overnight preculture of the best expression recombinant yeast was used to inoculate 1 L of glycerol complex medium (1% yeast extract, 2% peptone, 100 mM potassium phosphate buffer, pH 6.0, 1.34% yeast nitrogen base, 4×10^{-5}% biotin, 3% glycerol) and incubated for 2 days at 30°C in three 3-L baffle flasks. The cells were harvested by centrifugation (1500 × *g*, 10 min) and resuspended in a buffered 250-mL methanol complex medium (1% yeast extract, 1% peptone, 100 mM potassium phosphate buffer, pH 6.0, 1.34% yeast nitrogen base, 4×10^{-5}% biotin, 1% methanol) for 4 days at 30°C in twelve 1-L baffle flasks. An additional 1% methanol was added at 12-h intervals. The secreted rHSA dimer was purified on a Blue Sepharose CL-6B column (Amersham Biosciences). Isolated protein was defatted using the charcoal procedure described by Chen (12), deionized, freeze dried, and then stored at –20°C until use. N-terminal amino acid sequences of rHSA dimer were determined using a Perkin-Elmer ABI 477A protein sequencer.

Fluorescence and CD Spectra Measurements

Intrinsic fluorescence spectra of the proteins were measured using a Jasco FP-777 spectrofluorometer (Tokyo, Japan) equipped with thermostatically controlled 1-cm quartz cells and 5-nm excitation and emission bandwidths. Native HSA and the rHSA dimer were excited at 295 nm, and the spectra were corrected for buffer baseline fluorescence. CD spectra were obtained using a JASCO J-720 spectropolarimeter (JASCO, Tokyo, Japan) at 25°C. Far- and near-UV CD spectra were recorded at protein concentrations of 5 μM (native HSA) and 2.5 μM (rHSA dimer) and at 15 μM (native HSA) and 7.5 μM (rHSA dimer), respectively, in 67 mM phosphate buffer (pH 7.4).

SDS-PAGE and Western Blot Analysis

The rHSA dimer was analyzed via SDS-PAGE, using 8% polyacrylamide gel, and detected by staining with Coomassie blue. Western blotting was performed using an anti-HSA antibody raised in a rabbit as the primary antibody followed by an antirabbit secondary antibody conjugated to horseradish peroxidase. Proteins were detected using an enhanced chemiluminescence detection kit.

In Vivo Experiments: Animals

Male Wistar rats (5 weeks old, 150–170 g) and male ddY mice (6 weeks old, 28–30 g) were purchased from the Kyudou Co. (Kumamoto, Japan) and Japan SLC, Inc. (Shizuoka, Japan), respectively. The animals were maintained under conventional housing conditions, with free access to water and

food throughout the experimental period, and allowed to acclimatize to the laboratory environment for 1 week. After 1 week (1 week before injection of labeled protein), rats injected with ^{111}In-labeled protein were given water, which contains 5 mM sodium iodide, until the end of the experiment. All animal experiments were undertaken according to the guideline principles and procedures of Kumamoto University for the care and use of laboratory animals.

Radiolabeling with ^{125}I

Native HSA and rHSA dimer were labeled with ^{125}I using the Iodo-gen (1,3,4,6-tetrachoro-3a,6a-diphenylglycoluri) method (14). Nonincorporated ^{125}I was removed using a PD-10 column (Amersham Biosciences). ^{125}I-labeled protein was eluted from PD-10 column with phosphate-buffered saline (PBS). The derivative solution was concentrated and washed with saline by ultrafiltration.

Radiolabeling with ^{111}In

For the tissue distribution experiments, native HSA and rHSA dimer were radiolabeled with ^{111}In using the bifunctional chelating agent diethylenetriaminepentaacetic acid (DTPA) anhydride according to the method of Hnatowich *et al.* (15). In a typical experiment, each sample (5 mg) was dissolved in 1 mL 0.1 M 4-(2-Hydroxyethyl)-1-piperazineethanesulfonic acid (HEPES) buffer, pH 7, and mixed with 15 mM DTPA anhydride in 10 μL dimethyl sulfoxide. The mixture was stirred for 15 min at room temperature, and the radiolabeled product was purified by gel filtration using a Sephadex G-25 column (Amersham Biosciences) to remove unreacted DTPA. Fractions containing the sample were collected and concentrated by ultrafiltration at 4°C. A 20-μL aliquot of an $^{111}InCl_3$ solution (37 MBq/mL) was then added to 20 μL of 0.1 M citrate buffer, pH 5.5, and 40 μL of a DTPA-coupled derivative solution was added to the mixture. After 15 min, the mixture was applied to a PD-10 column and eluted with 0.1 M citrate buffer, pH 5.5. The derivative fractions were collected and concentrated by ultrafiltration at 4°C (16).

Pharmacokinetic Analysis

Iodination proteins (1.0×10^8 cpm/kg, 0.1 mg/kg) in saline were injected into the tail vein of male Wistar rats. Blood (100 μL) samples were periodically collected from the tail vein using a heparinized needle at 1, 5, 10, 20, 30, and 45 min and at 1, 2, 4, 8, 12, 18, 24, 36, 48, 60, 72, 84, and 96 h, and plasma was obtained by centrifugation. The radioactivity of plasma (20 μL) samples was determined using a γ-counter (ARC-380; Aloka, Tokyo, Japan); 1 mL of 1% bovine serum albumin was then added to the plasma followed by 1 mL of 40% TCA. The sample was incubated with stirring for 10 min. After the incubation, the sample was centrifuged and the radioactivity in the pellet was recounted on the γ-counter. Urine and feces were collected at 24-h intervals, and blood was collected from other rats that were kept in a metabolic cage. The area under the plasma concentration–time curve (AUC) was calculated by fitting an equation to the plasma precipitated by TCA concentrations of the derivatives using MULTI, a nonlinear least-squares program (17).

Biodistribution Experiment

We injected ^{111}In-protein into the tail vein of male ddY mice. At 1, 4, 12, and 24 h after injection of these radiolabeled proteins, the percentage of the injected dose (%ID) per gram or milliliter of several tissues was estimated (13). Male ddY mice received a 0.1-mg/kg dose (16.7×10^6 cpm/kg) of ^{111}In-native HSA or ^{111}In-rHSA dimer conjugate in saline by injection into the tail vein. At 1, 4, 12, and 24 h after injection of these radiolabeled proteins, blood was collected from the vena cava with the animal under ether anesthesia, and plasma was obtained by centrifugation. At each of these time points, an animal was killed for excision of kidney, liver, spleen skin, muscle, and fat. These organs were then rinsed with saline and weighed, and the radioactivity contained by the samples was determined. ^{111}In radioactivity was counted using a γ-counter (ARC-5000; Aloka).

Carrageenin-Induced Paw Edema

Paw edema was induced by the subcutaneous injection of 50 μL of a saline solution containing 0.4% carrageenin into the right paw of male ddY mice, and 50 μL of saline solution alone was injected to the left paw as a control. The time of carrageenin injection was designated as time 0. After the carrageenin injection, the mice were injected with a 0.1-mg/kg dose (16.7×10^6 cpm/kg) of ^{125}I-native HSA or ^{125}I-rHSA dimer into a tail vein at different time points. The mice were exsanguinated to death 15 min after the injection of radiolabeled protein. Both paws were removed, and the radioactivity in each paw was measured. Footpad thickness was measured twice immediately before the injection of carrageenin and the radiolabeled protein with a thickness

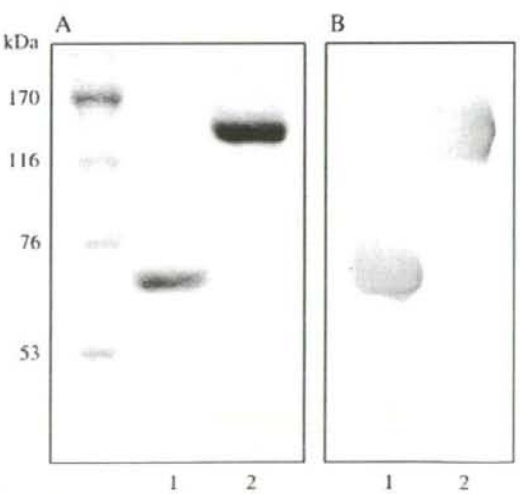

Fig. 2. Sodium dodecyl sulfate polyacrylamide gel electrophoresis (A) and Western blot analysis (B) of native HSA and rHSA dimer. Lane 1, native HSA; lane 2, rHSA dimer (3 μg per lane).

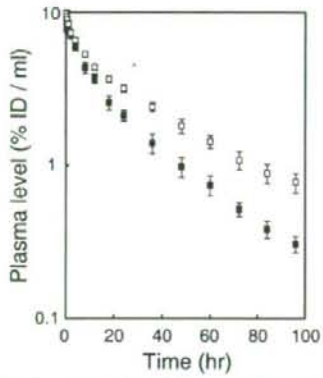

Fig. 3. Plasma level of radiolabeled proteins after intravenous administration of ^{125}I-native HSA (filled symbol) or ^{125}I-rHSA dimer (open symbol) to normal rats. Each point represents the mean ± SD (n = 4). %ID, percentage of injected dose.

gage 7301 (Mitutoyo, Kanagawa, Japan). Paw edema was expressed in terms of the difference in footpad thickness between the right and the left paw.

Carrageenin Air Pouch

Inflammation of the carrageenin air pouch was induced according to the method of Tsurufuji (18). Male Wistar rats, 6 weeks of age and weighing 180–200 g, were subcutaneously injected, under light ether anesthesia, with 8.0 mL of air on the back to create an air pouch. After 24 h, 4.0 mL of a 2% (w/v) carrageenin solution in 0.9% NaCl was injected into the air pouch that had been produced. The carrageenin solution was autoclaved at 120°C for 20 min and injected, after cooling, at a temperature of 40–45°C. Immediately before the injection, penicillin and streptomycin were added in a concentration of 0.1 mg/mL each to the carrageenin solution. After 6 days of carrageenin injection, 1.0×10^8 cpm/kg, 0.1 mg/kg ^{125}I-native HSA or ^{125}I-rHSA dimer was injected into a tail vein. The day of radiolabel protein injection was designated as day 0. Collection of blood, plasma, urine, and feces and a pharmacokinetic analysis followed the above method (*Pharmacokinetic Analysis*). The weight and radioactivity of the pouch fluid was measured after exsanguination of the rats to death.

Statistical Analysis

All data are presented as mean ± SD. Significant differences between native HSA and rHSA dimer were tested by Student's t test.

RESULTS

Cloning and Expression of rHSA Dimer

The rHSA dimer was expressed using *P. pastoris*. The HSA sequence contains 585 amino acids. The rHSA dimer was designed to contain two sets of the 585 amino acids fused with a linker of 10 amino acid $(GGGGS)_2$. The polypeptide linker is flexible and highly hydrophilic and, hence, is resistant to proteases (19,20). Construction of the expression vector of the rHSA dimer was made by a four-piece ligation (Fig. 1). The reason for the four-piece ligation was that pPIC9K cannot be used directly due to the presence of the *Xho*I restriction site in the kanamycin resistance gene. Furthermore, the use of other restriction enzymes would result in the addition of some other amino acids in the expressed protein. Although there is another alternative for using pPIC9, which does not contain a kanamycin resistance gene, pPIC9K is easier than pPIC9 in the selection of a high-expression strain. The N-terminal amino acid sequence of the rHSA dimer expressed in the present study was found to be consistent with that of native HSA.

Structural Aspects of rHSA Dimer

Sodium dodecyl sulfate polyacrylamide gel electrophoresis of the rHSA dimer showed a single band, and the dimer protein was recognized by an anti-HSA antibody. As shown in Fig. 2, the molecular weight of rHSA dimer (~13 kDa) was approximately twice the molecular weight of native HSA in SDS-PAGE. The intrinsic fluorescence spectra of Trp-214, the only tryptophan residue of HSA, in the rHSA dimer was slightly low compared with that of native HSA (data not shown). To obtain information on secondary and tertiary protein structures, CD measurements were performed in the far-UV and near-UV regions (data not shown). A little decrease in the molar ellipticity of the rHSA dimer was observed in comparison with that of native HSA in the far-UV CD spectrum. Although some spectral changes were observed, the near-UV CD spectra of the rHSA dimer show the same minima and shape as that of native HSA. These results suggest that the rHSA dimer structure is almost identical to that of native HSA.

Pharmacokinetic Analysis of rHSA Dimer

Pharmacokinetics of the ^{125}I-labeled native HSA and rHSA dimer was evaluated by residual TCA-precipitable plasma radioactivity. Figure 3 shows the time courses of plasma concentration of radiolabeled rHSA dimer and native HSA, and the pharmacokinetic parameters for these two proteins using a two-compartment model are listed in Table I.

Table I. Pharmacokinetic Parameters After an Intravenous Administration of ^{125}I-native HSA or ^{125}I-rHSA Dimer to Normal Rats

	AUC (min x %ID/mL)	CL_{tot} (μL/h)	Vd_{ss} (mL)	$T_{1/2}$, β (h)
^{125}I-native HAS	154.6 ± 15.5	654.6 ± 65.0	20.01 ± 1.35	26.19 ± 0.74
^{125}I-rHSA dimer	265.6 ± 15.2†	380.1 ± 25.6†	18.13 ± 1.36	36.53 ± 1.14*

All values are mean ± SD (n = 4).
*$p < 0.005$, † $p < 0.001$ *vs.* ^{125}I-HSA native.

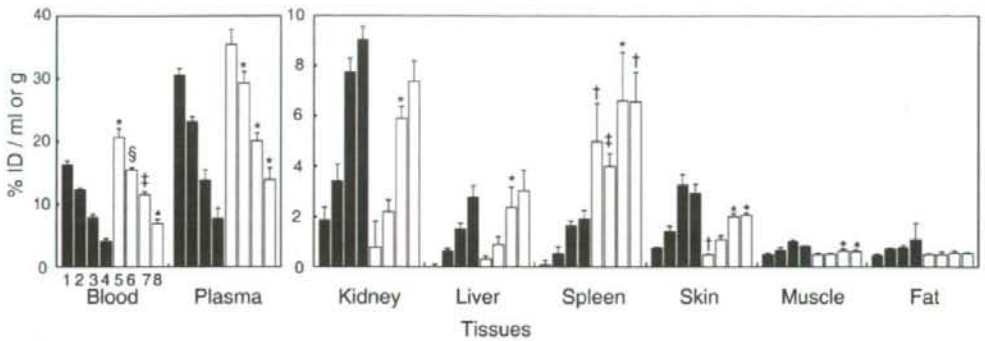

Fig. 4. Tissue distribution of ^{111}In-native HSA (filled bar) and ^{111}In-rHSA dimer (open bar) at 1, 4, 12, and 24 h after an intravenous administration to normal mice. Lanes 1 and 5, 1 h; lanes 2 and 6, 4 h; lanes 3 and 7, 12 h; lanes 4 and 8, 24 h. Each bar represents the mean ± SD (n = 3). $^{*}p < 0.05$, $^{\dagger}p < 0.01$, $^{\ddagger}p < 0.005$, $^{\S}p < 0.001$ *vs.* ^{125}I-native HSA.

The AUC and half-life of the ^{125}I-rHSA dimer were increased by about 1.5 times, as compared with those of ^{125}I-native HSA. On the other hand, the ^{125}I-rHSA dimer showed a two-thirds decrease in total body clearance (CL_{tot}), and a decline in the distribution volume of the steady state (Vd_{ss}) was observed. These results suggest that the ^{125}I-rHSA dimer has a better retention in the blood circulation, as compared with ^{125}I-native HSA.

Biodistribution of rHSA Dimer

The tissue distribution of ^{111}In-labeled protein was examined in the mouse (Fig. 4). The retention of the ^{111}In-rHSA dimer in the blood and plasma was confirmed when compared with the ^{111}In-native HSA. The accumulation of the ^{111}In-rHSA dimer in the kidney was significantly lower only after 12 and 24 h. The accumulation of the ^{111}In-rHSA dimer in the liver was significantly higher at 12 h. The accumulation of the ^{111}In-rHSA dimer in the skin, muscle, and fat was lower, with a significant decrease observed in the skin and muscle. In contrast, no significant difference was observed for the ^{111}In-rHSA dimer in the urine and feces (Table II). The urine at 24 and 96 h from a mouse administered with the ^{111}In-rHSA dimer and ^{111}In-native HSA, respectively, was ultrafiltrated. More than 98% of the filtrate was composed of low molecular substances under 30,000 in molecular weight, and the excretion of high molecular weight protein was negligible. Ultrafiltration of the plasma containing the ^{111}In-rHSA dimer and ^{111}In-native HSA obtained at 1 h showed that more than 99% existed as high molecular weight protein.

Vascular Permeability of rHSA Dimer

The vascular permeability of the ^{125}I-rHSA dimer was evaluated using carrageenin-induced mouse paw edema as a model system (Fig. 5). Carrageenin-induced mouse paw edema is known to exhibit a biphasic inflammatory response (21). In this study, the biphasic response was confirmed by measurements of the increase in the thickness of the foot. The vascular permeability of the ^{125}I-rHSA dimer was low between 0.5 and 120 h, especially at 0.5, 1, 4, 8, 24, 48, and 96 h where a significantly low permeability was observed compared with that of ^{125}I-native HSA. These results suggest that the escape of HSA to the extravascular space during inflammation can be reduced by dimerization.

Pharmacokinetic Analysis of rHSA Dimer in Carrageenin-Air-Pouch Rats

Pharmacokinetics of ^{125}I-labeled native HSA and the rHSA dimer in carrageenin-air-pouch rats was evaluated by measuring the residual TCA-precipitable plasma radioactivity. Table III shows the results of an analysis of the pharmacokinetic parameters using a two-compartment model. This model also showed an improvement in the retention of ^{125}I-rHSA dimer in the blood. A significant difference in half-life of the β phase could be observed; the AUC for the ^{125}I-rHSA dimer was 1 1/2 times larger, whereas the CL_{tot} value was 2/3 times smaller, as compared with ^{125}I-native HSA. The Vd_{ss} for the ^{125}I-rHSA dimer showed a significantly lower value than that of ^{125}I-native HSA as well. Urine and feces were collected at 24-h intervals from rats

Table II. Urinary and Fecal Excretion of Radioactivity After an Intravenous Administration of ^{111}In-native HSA or ^{111}In-rHSA Dimer

	Urine (%ID)		Feces (%ID)	
	12 h	24 h	12 h	24 h
^{111}In-native HAS	1.65 ± 0.02	3.37 ± 1.08	0.82 ± 0.15	1.43 ± 0.06
^{111}In-rHSA dimer	1.74 ± 0.37	2.67 ± 0.36	0.68 ± 0.20	1.32 ± 0.18

All values are mean ± SD (n = 3).

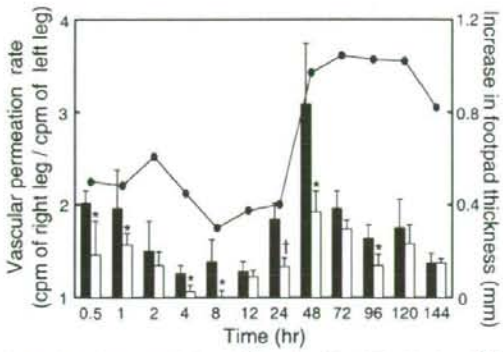

Fig. 5. Vascular permeability of ^{125}I-native HSA (filled bar) and ^{125}I-rHSA dimer (open bar) in mouse models of paw edema. A line graph shows the increase in footpad thickness. The data are the average values of five to seven experiments (±SD). $^{*}p < 0.05$, $^{\dagger}p < 0.01$ *vs.* ^{125}I-native HSA.

different from those used for blood collection kept in metabolic cages (Table IV). According to the comparison between rats administered with the same proteins, the air-pouch model rat showed a greater decrease in the early excretion in both ^{125}I-native HSA and the ^{125}I-rHSA dimer than normal rats. In addition, the 96-h alveolar activity of rats kept in the metabolic cage was determined. No significant difference in the weight of alveolar fluid was found between ^{125}I-native HSA and the ^{125}I-rHSA dimer (Table V).

DISCUSSION

Intravascular fluid therapy is a common critical care intervention. Many fluids have been studied for use in resuscitation, and these include isotonic sodium chloride solution, lactated Ringer solution, hypertonic saline, albumin, purified protein fractions, freshly frozen plasma, hetastarch, pentastarch, and dextran 70. In spite of the many theoretical benefits of human albumin administration in critically ill patients, there has been little evidence to support its widespread clinical use. Previous systematic reviews have produced conflicting results regarding the safety and efficacy of the use of albumin (2,22). The recently reported saline *vs.* albumin evaluation study has provided conclusive evidence that 4% albumin is as safe as saline for resuscitation, although no overall benefit of albumin use was reported (3,23). Albumin solutions for resuscitation may still be warranted in certain highly selected patient populations such as liver transplant patients and burn patients.

Albumin plays an important role in the circulation by generating an inward oncotic force that counteracts the outward capillary hydrostatic force. Without albumin, plasma volume cannot be maintained and massive interstitial edema results. In burn shock, in which the effective circulation is reduced, albumin and extracellular fluid are rapidly shifted from the plasma and sequestered in interstitial fluids. It is commonly thought that the permeability of the capillary membranes is pathologically increased in states of shock. Burn injury is also characterized by a dramatic increase in capillary protein permeability. When shock does not develop in small burns, or is prevented by fluid therapy, the rate of protein extravasation may increase to up to 100 times the normal rate. Mechanisms that regulate plasma albumin content are the transcapillary escape rate of albumin (TER_{alb}), lymphatic albumin return, and the albumin synthesis-to-degradation ratio. TER_{alb} measures the whole body rate at which albumin leaves the vascular space. It is controlled by macrovascular and microvascular factors including plasma albumin concentration, plasma atrial natriuretic peptide concentration, capillary filtration coefficient, capillary hydrostatic pressure, interstitial fluid hydrostatic pressure, interstitial fluid colloid osmotic pressure, and interstitial fluid albumin concentration (24,25).

Albumin leaves the circulation via several mechanisms, which vary with the tissue involved. In organs having sinusoids, i.e., liver and bone marrow, plasma can pass through large gaps in the endothelium. Some other organs have fenestrated endothelia that allow unimpeded passage; the pancreas, small intestine, and adrenal gland are examples of these. Collectively, these convection mechanisms account for about 50% of albumin transport from the circulation. The transport may be described as taking place through two sets of parallel and cylindrical pores, one set with diameters of 45–60 Å and another with a diameter of ~200 Å. It has been shown that albumin, with an estimated radius of 35.5 Å, and water do not share a common pathway in crossing the endothelial monolayer, suggesting the existence of a large pore pathway for albumin (26). Results reported by Sejrsen *et al.* (27) indicate that the predominant transcapillary transport mechanism for ^{131}I-albumin is compatible with transcapillary diffusion through pores with an effective equivalent pore radius of 145 Å. Hence, the extent of extravasation of albumin may be reduced by increasing its molecular size.

In this study, we attempted to express an rHSA dimer by fusing two HSA molecules, containing two sets of the protein sequence of 585 amino acids, linked with an amino acid linker $(GGGGS)_2$. As can be inferred from the intrinsic fluorescence spectra and CD spectra, the structural characteristics of the rHSA dimer are almost identical to that of

Table III. Pharmacokinetic Parameters After an Intravenous Administration of ^{125}I-native HSA or ^{125}I-rHSA Dimer to Carrageenin-Air-Pouch Rats

	AUC (min x %ID/mL)	CL_{tot} (μL/h)	Vd_{ss} (mL)	$T_{1/2}$, β (h)
^{125}I-native HAS	103.1 ± 5.3	974.6 ± 53.2	22.38 ± 1.01	24.85 ± 0.55
^{125}I-rHSA dimer	164.0 ± 10.1‡	612.9 ± 36.4‡	19.47 ± 1.09†	27.30 ± 1.40*

All values are mean ± SD ($n = 5$).
$^{*}p < 0.05$, $^{\dagger}p < 0.01$, $^{\ddagger}p < 0.001$ *vs.* ^{125}I-native HSA.

Table IV. Radioactivity in Pouch Fluid After an Intravenous Administration of ^{125}I-native HSA or ^{125}I-rHSA Dimer to Carrageenin-Air-Pouch Rats at 96 h

	Pouch fluid (g)	Radioactivity (%ID)
^{125}I-native HSA	40.57 ± 2.19	11.12 ± 1.60
^{125}I-rHSA dimer	44.10 ± 2.30	13.58 ± 0.19

All values are mean ± SD (n = 4).

native HSA. The pharmacokinetic analysis of the rHSA dimer indicated that, in general, the rHSA dimer showed longer intravascular residence time, as compared with native HSA. (Fig. 3 and Table I). A biodistribution analysis of the rHSA dimer generally showed a similar tendency with that of the native HSA except for the fact that the extent of accumulation of the rHSA dimer in the spleen was much greater, whereas in the skin and muscle, the accumulation was less than that of native HSA (Fig. 4). This observation is in agreement with the findings reported by Rennen *et al.* (28), in which a rapid blood clearance with predominant uptake by the liver and spleen was found for the largest proteins (MW 669–800 kDa), a relatively slow blood clearance with relatively moderate uptake by the liver and spleen was seen for proteins of intermediate size (MW 66–206 kDa), and a rapid blood clearance with predominant kidney uptake was found for smaller proteins (MW 2.5–29 kDa). However, it is noteworthy that the blood retention properties of the rHSA dimer were higher in comparison with native HSA (Table I). In contrast, no significant difference could be observed for the rHSA dimer and native HSA in terms of excretion in the urine and feces (Table II).

HSA is not degraded by a specific organ but by many organs such as the liver, kidney, skin, and muscle. The binding of albumin to the endothelial surface apparently initiates its transcytosis via plasmalemmal vesicles and also increases capillary permselectivity. Scavenger receptors interact with a variety of modified proteins, mediate their endocytosis and degradation, and may play an important role in protein catabolism and pathogenic processes such as atherosclerosis, aging, and diabetes. Specific albumin binding to the surface of the endothelium initiates its transcytosis across the continuous endothelium via noncoated plasmalemmal vesicles. Previous studies have identified several putative albumin-binding proteins (SPARC, gp60, gp30, and gp18). Two membrane-associated proteins, gp30 and gp18, interact more strongly with albumins that have been conformationally modified by chemical means or by surface adsorption to colloidal gold particles than with native albumin. The gp30 and gp18 proteins behave similarly to other known scavenger receptors, suggesting that gp30 and gp18 may mediate the high-affinity binding, endocytosis, and degradation of conformationally modified albumins but not native albumin, whereas albondin mediates native albumin binding, which significantly enhances its transcytosis and capillary permeability (29,30).

On the other hand, the effect of an increase in vascular permeability during inflammation on the vascular permeability of the rHSA dimer was evaluated using carrageenin-induced paw edema in mice (Fig. 5). This carrageenin-induced inflammation can be used to evaluate acute exudative stage and chronic proliferative stage of carrageenin-air-pouch inflammation in rats (31). Up to 120 h, the vascular permeability of the rHSA dimer was less than that of native HSA in the model mice. In particular, significant difference was observed during the acute inflammation stage. In addition, the pharmacokinetics of the rHSA dimer was evaluated in carrageenin-air-pouch rats (Table III). Similar profile has been obtained for the pharmacokinetics of the rHSA dimer in the inflammation mouse model as in the normal rats. In comparison with native HSA, longer blood retention and lower vascular permeability of the rHSA dimer were shown by the pharmacokinetic and vascular permeability analyses.

In contrast to our observations, McCurdy *et al.* (32) showed that a recombinant rabbit albumin (RSA) dimer consisting of N-terminal hexahistidinyl tagRSA(C34A) joined to G6 joined to RSA containing the C34A mutation in that order, from the N-terminus to the C-terminus, is more rapidly cleared *in vivo* than wild-type and mutant C34A rabbit albumins. The authors concluded from their study that albumin dimerization does not look promising as a tool to slow clearance. They deduced that the mechanism of the accelerated clearance of recombinant rabbit serum albumin appears to involve the reticuloendothelial system. On the other hand, Komatsu *et al.* (33) has demonstrated the utility of an rHSA dimer, which was cross-linked by the thiol group of Cys-34 with 1,6-bis(maleimido)hexane, and its synthetic heme hybrid as an oxygen carrier displayed a longer half-life in the bloodstream and tissue distributions that were similar to rHSA. The discrepancy between the studies may probably due to species difference, as shown in the study by Sheffield *et al.* (34).

Table V. Urinary and Fecal Excretion of Radioactivity (%ID) After an Intravenous Administration of ^{125}I-native HSA or ^{125}I-rHSA Dimer to Normal or Carrageenin-Air-Pouch Rats

	Excretion of radioactivity (%ID)							
	^{125}I-native HSA				^{125}I-rHSA dimer			
	Normal		Air pouch		Normal		Air pouch	
Time (h)	Urine	Feces	Urine	Feces	Urine	Feces	Urine	Feces
0–24	39.7 ± 0.8	1.54 ± 0.42	43.5 ± 4.7	1.58 ± 0.54	35.0 ± 1.5	1.67 ± 0.35	44.8 ± 2.0	1.51 ± 0.41
24–48	25.9 ± 3.2	1.96 ± 0.44	20.7 ± 2.2	1.69 ± 0.36	19.7 ± 0.5	1.34 ± 0.20	18.2 ± 1.6	1.22 ± 0.12
48–72	13.0 ± 0.7	1.03 ± 0.21	8.5 ± 0.5	0.54 ± 0.15	11.2 ± 0.6	0.79 ± 0.24	8.04 ± 0.6	0.53 ± 0.13
72–96	6.1 ± 0.3	0.52 ± 0.05	5.1 ± 0.3	0.40 ± 0.01	7.2 ± 0.4	0.47 ± 0.01	3.6 ± 0.4	0.26 ± 0.02

All values are mean ± SD (n = 4).

Indeed, the clearance of albumin depends on various factors including its degradation by a variety of organs, transcapillary escape, filtration and reabsorption, and lymphatic drainage, just to name a few. These pathways in turn are also influenced by the physicochemical state of the protein, such as its charge and conformation. In skin, the clearance for the most neutral modified albumins and cationic albumins was found to be 20 and 80% greater than that for native albumin, respectively. In skeletal muscle, the clearance for the most neutral modified albumins and cationic albumins was found to be 50 and 150% greater than that for native albumin, respectively. This clearly shows that charge affects the transvascular transport of albumin (35,36). In this study, the fusion has been carried out through the N- and C-terminals. Since no conjugation of any of the amino acid residues has taken place, the charge of the rHSA dimer should be the same as the native HSA (monomer albumin). In addition, environmental factors such as the presence of nitric oxide have also been reported to influence the extravasation of albumin (37).

Collectively, an increase in the molecular size of HSA probably prevents or retards its convection movement through pores with diameters of 45–60 Å, as observed by an increase in AUC and a decrease in the volume of distribution as well as the clearance of the dimer. Meanwhile, since the dimer exhibits structural features similar to those of native albumin, we hypothesize that transvascular movement of the rHSA dimer takes place via the same route, i.e., gp60, as evidenced by the similarity in tissue distribution profile. However, further research must be carried out to validate such speculation.

On the other hand, since HSA is an endogenous protein, it has been developed for use as a drug carrier due to its excellent biological compatibility. A promising outcome has also been reported using recombinant albumin as a synthetic heme carrier protein in producing artificial blood (38,39). It is noteworthy that albumin has recently been used as a carrier to prolong the blood retention properties of therapeutic proteins such as interferon and growth hormone. Through genetic fusion technology, the therapeutic protein is fused to albumin and, as a result, the plasma half-life of the protein becomes dependent on the half-life of albumin (40–45). Fusion to albumin offers several advantages. Albumin is the most abundant protein in mammalian plasma and one of the longest lived. It lacks posttranslational modifications, with the exception of extensive disulfide bonding. If albumin can be fused in-frame with a therapeutic protein as a single-chain polypeptide, the novel protein may acquire the slow clearance profile of albumin, while retaining the activity important for clinical use. On the other hand, although conjugation of polyethylene glycol with the protein may also produce similar tendency, such approach involves modification of the internal amino acid side chain, which may change the charge distribution and, hence, affect the stability of the protein. Albuferon (albumin-interferon alpha) exhibits more antiviral activity at clinically achieved serum levels than standard interferon alpha or the modified interferons, Pegasys (peginterferon alpha-2a) and Peg-Intron (peginterferon alpha-2b) (43).

Clinical and preclinical results to date demonstrate that Albuferon is well tolerated, with adverse events that are transient and mostly mild to moderate in severity, and exhibits a robust antiviral activity, with a pharmacokinetic profile that supports dosing at intervals of 2 to 4 weeks. This prolongation in half-life prevents the frequent administration of the therapeutic protein. Hence, although albumin genetic fusion technology is very promising, if the blood retention properties of albumin can be improved further, it is expected that such albumin will be of great clinical use as a new drug delivery system material in addition to being a plasma expander.

ACKNOWLEDGMENTS

We wish to thank the members of the Gene Technology Center in Kumamoto University for their important contributions to these experiments.

REFERENCES

1. T. Peters. *All About Albumin: Biochemistry, Genetics, and Medical Applications*, Academic, San Diego, 1996.
2. Cochrane Injuries Group. Human albumin administration in critically ill patients: systematic review of randomised controlled trials. Cochrane Injuries Group Albumin Reviewers. *BMJ* **317**: 235–240 (1998).
3. S. Finfer, R. Bellomo, N. Boyce, J. French, J. Myburgh, and R. Norton. A comparison of albumin and saline for fluid resuscitation in the intensive care unit. *N. Engl. J. Med.* **350**:2247–2256 (2004).
4. H. Rubin, S. Carlson, M. DeMeo, D. Ganger, and R. M. Craig. Randomized, double-blind study of intravenous human albumin in hypoalbuminemic patients receiving total parenteral nutrition. *Crit. Care Med.* **25**:249–252 (1997).
5. G. Akerstrom and B. Lisander. Tissue extravasation of albumin from intraabdominal trauma in rats. *Acta Anaesthesiol. Scand.* **35**:257–261 (1991).
6. M. P. Margarson and N. C. Soni. Tissue extravasation of albumin from intraabdominal trauma in rats. *Br. J. Anaesth.* **92**:821–826 (2004).
7. S. Berg, M. Golster, and B. Lisander. Albumin extravasation and tissue washout of hyaluronan after plasma volume expansion with crystalloid or hypooncotic colloid solutions. *Acta Anaesthesiol. Scand.* **46**:166–172 (2002).
8. M. Mathru, B. Blakeman, D. J. Dries, B. Kleinman, and P. Kumar. Permeability pulmonary edema following lung resection. *Chest* **98**:1216–1218 (1990).
9. K. Byrne, J. L. Tatum, D. A. Henry, J. I. Hirsch, M. Crossland, T. Barnes, J. A. Thompson, J. Young, and H. J. Sugerman. Increased morbidity with increased pulmonary albumin flux in sepsis-related adult respiratory distress syndrome. *Crit. Care Med.* **20**:28–34 (1992).
10. S. Galatius, L. Bent-Hansen, H. Wroblewski, V. B. Sorensen, T. Norgaard, and J. Kastrup. Plasma disappearance of albumin and impact of capillary thickness in idiopathic dilated cardiomyopathy and after heart transplantation. *Circulation* **102**:319–325 (2000).
11. T. Oshima, F. S. Laroux, L. L. Coe, Z. Morise, S. Kawachi, P. Bauer, M. B. Grisham, R. D. Specian, P. Carter, S. Jennings, D. N. Granger, T. Joh, and J. S. Alexander. Interferon-gamma and interleukin-10 reciprocally regulate endothelial junction integrity and barrier function. *Microvasc. Res.* **61**:130–143 (2001).
12. R. F. Chen. Removal of fatty acids from serum albumin by charcoal treatment. *J. Biol. Chem.* **242**:173–181 (1967).
13. S. Matsushita, Y. Isima, V. T. Chuang, H. Watanabe, S. Tanase, T. Maruyama, and M. Otagiri. Functional analysis of recombinant human serum albumin domains for pharmaceutical applications. *Pharm. Res.* **21**:1924–1932 (2004).
14. J. Bhatia, S. K. Sharma, K. A. Chester, R. B. Pedley, R. W. Boden, D. A. Read, G. M. Boxer, N. P. Michael, and R. H. Begent. Catalytic activity of an *in vivo* tumor targeted anti-CEA scFv::carboxypeptidase G2 fusion protein. *Int. J. Cancer* **85**:571–577 (2000).

15. D. J. Hnatowich, W. W. Layne, and R. L. Childs. The preparation and labeling of DTPA-coupled albumin. *Int. J. Appl. Radiat. Isot.* **33**:327–332 (1982).
16. H. Katsumi, M. Nishikawa, S. F. Ma, F. Yamashita, and M. Hashida. Physicochemical, tissue distribution, and vasodilation characteristics of nitrosated serum albumin: delivery of nitric oxide *in vivo*. *J. Pharm. Sci.* **93**:2343–2352 (2004).
17. K. Yamaoka, Y. Tanigawara, T. Nakagawa, and T. A. Uno. Pharmacokinetic analysis program (multi) for microcomputer. *J. Pharmacobio-dyn.* **4**:879–885 (1981).
18. S. Tsurufuji, H. Sato, K. R. Min, and K. Ohuchi. Difference in the anti-inflammatory effect of indomethacin between acute and chronic stages of carrageenin-induced inflammation. *J. Pharmacobio-dyn.* **1**:8–14 (1978).
19. D. Shan, O. W. Press, T. T. Tsu, M. S. Hayden, and J. A. Ledbetter. Characterization of scFv-Ig constructs generated from the anti-CD20 mAb 1F5 using linker peptides of varying lengths. *J. Immunol.* **162**:6589–6595 (1999).
20. M. Gustavsson, J. Lehtio, S. Denman, T. T. Teeri, K. Hult, and M. Martinelle. Stable linker peptides for a cellulose-binding domain-lipase fusion protein expressed in Pichia pastoris. *Protein Eng.* **14**:711–715 (2001).
21. I. Posadas, M. Bucci, F. Roviezzo, A. Rossi, L. Parente, L. Sautebin, and G. Cirino. Carrageenan-induced mouse paw oedema is biphasic, age-weight dependent and displays differential nitric oxide cyclooxygenase-2 expression. *Br. J. Pharmacol.* **142**:331–338 (2004).
22. M. M. Wilkes and R. J. Navickis. Patient survival after human albumin administration. A meta-analysis of randomized, controlled trials. *Ann. Intern. Med.* **135**:149–164 (2001).
23. E. Fan and T. E. Stewart. Albumin in critical care: SAFE, but worth its salt? *Crit. Care* **8**:297–299 (2004).
24. B. Rippe and B. Haraldsson. Transport of macromolecules across microvascular walls: the two-pore theory. *Physiol. Rev.* **74**:163–219 (1994).
25. C. C. Michel and F. E. Curry. Microvascular permeability. *Physiol. Rev.* **79**:703–761 (1999).
26. R. O. Dull, H. Jo, H. Sill, T. M. Hollis, and J. M. Tarbell. The effect of varying albumin concentration and hydrostatic pressure on hydraulic conductivity and albumin permeability of cultured endothelial monolayers. *Microvasc. Res.* **41**:390–407 (1991).
27. P. Sejrsen, W. P. Paaske, and O. Henriksen. Capillary permeability of 131I-albumin in skeletal muscle. *Microvasc. Res.* **29**: 265–281 (1985).
28. H. J. Rennen, J. Makarewicz, W. J. Oyen, P. Laverman, F. H. Corstens, and O. C. Boerman. The effect of molecular weight on nonspecific accumulation of (99m)T-labeled proteins in inflammatory foci. *Nucl. Med. Biol.* **28**:401–408 (2001).
29. J. E. Schnitzer, A. Sung, R. Horvat, and J. Bravo. Preferential interaction of albumin-binding proteins, gp30 and gp18, with conformationally modified albumins. Presence in many cells and tissues with a possible role in catabolism. *J. Biol. Chem.* **267**:24544–24553 (1992).
30. J. E. Schnitzer and P. Oh. Albondin-mediated capillary permeability to albumin. Differential role of receptors in endothelial transcytosis and endocytosis of native and modified albumins. *J. Biol. Chem.* **269**:6072–6082 (1994).
31. H. Sato, M. Hashimoto, K. Sugio, K. Ohuchi, and S. Tsurufuji. Comparative study between steroidal and nonsteroidal anti-inflammatory drugs on the mode of their actions on vascular permeability in rat carrageenin-air-pouch inflammation. *J. Pharmacobio-dyn.* **3**:345–352 (1980).
32. T. R. McCurdy, S. Gataiance, L. J. Eltringham-Smith, and W. P. Sheffield. A covalently linked recombinant albumin dimer is more rapidly cleared *in vivo* than are wild-type and mutant C34A albumin. *J. Lab. Clin. Med.* **143**:115–124 (2004).
33. T. Komatsu, Y. Oguro, Y. Teramura, S. Takeoka, J. Okai, M. Anraku, M. Otagiri, and E. Tsuchida. Physicochemical characterization of cross-linked human serum albumin dimer and its synthetic heme hybrid as an oxygen carrier. *Biochim. Biophys. Acta* **1675**:21–31 (2004).
34. W. P. Sheffield, A. Mamdani, G. Hortelano, S. Gataiance, L. Eltringham-Smith, M. E. Begbie, R. A. Leyva, P. S. Liaw, and F. A. Ofosu. Effects of genetic fusion of factor IX to albumin on *in vivo* clearance in mice and rabbits. *Br. J. Haematol.* **126**:565–573 (2004).
35. R. R. Gandhi and D. R. Bell. Importance of charge on transvascular albumin transport in skin and skeletal muscle. *Am. J. Physiol.* **262**:H999–H1008 (1992).
36. H. Vink and B. R. Duling. Capillary endothelial surface layer selectively reduces plasma solute distribution volume. *Am. J. Physiol, Heart Circ. Physiol.* **278**:H285–H289 (2000).
37. L. W. Chen, J. S. Wang, B. Hwang, J. S. Chen, and C. M. Hsu. Reversal of the effect of albumin on gut barrier function in burn by the inhibition of inducible isoform of nitric oxide synthase. *Arch. Surg.* **138**:1219–1225 (2003).
38. E. Tsuchida, K. Ando, H. Maejima, N. Kawai, T. Komatsu, S. Takeoka, and H. Nishide. Properties of and oxygen binding by albumin-tetraphenylporphyrinatoiron(II) derivative complexes. *Bioconjug. Chem.* **8**:534–538 (1997).
39. T. Komatsu, H. Yamamoto, Y. Huang, H. Horinouchi, K. Kobayashi, and E. Tsuchida. Exchange transfusion with synthetic oxygen-carrying plasma protein –albumin-heme– into an acute anemia rat model after seventy-percent hemodilution. *J. Biomed. Mater. Res., A.* **71**:644–651 (2004).
40. S. Syed, P. Schuyler, M. Kulczycky, and W. P. Sheffield. Potent antithrombin activity and delayed clearance from the circulation characterize recombinant hirudin genetically fused to albumin. *Blood* **89**:3243–3252 (1997).
41. P. Yeh, D. Landais, M. Lemaitre, I. Maury, J.-Y. Crenne, J. Becquart, A. Murry-Brelier, F. Boucher, G. Montay, R. Fleer, P.-H. Hirel, J.-F. Mayaux, and D. Klatzmann. Design of yeast-secreted albumin derivatives for human therapy: biological and antiviral properties of a serum albumin–CD4 genetic conjugate. *Proc. Natl. Acad. Sci. U. S. A.* **89**:1904–1908 (1992).
42. M. S. Dennis, M. Zhang, Y. G. Meng, M. Kadkhodayan, D. Kirchhofer, D. Combs, and L. A. Damico. Albumin binding as a general strategy for improving the pharmacokinetics of proteins. *J. Biol. Chem.* **277**:35035–35043 (2002).
43. B. L. Osborn, H. S. Olsen, B. Nardelli, J. H. Murray, J. X. Zhou, A. Garcia, G. Moody, L. S. Zaritskaya, and C. Sung. Pharmacokinetic and pharmacodynamic studies of a human serum albumin–interferon-alpha fusion protein in cynomolgus monkeys. *J. Pharmacol. Exp. Ther.* **303**:540–548 (2002).
44. C. Sung, B. Nardelli, D. W. LaFleur, E. Blatter, M. Corcoran, H. S. Olsen, C. E. Birse, O. K. Pickeral, J. Zhang, D. Shah, G. Moody, S. Gentz, L. Beebe, and P. A. Moore. An IFN-beta–albumin fusion protein that displays improved pharmacokinetic and pharmacodynamic properties in nonhuman primates. *J. Interferon Cytokine Res.* **23**:25–36 (2003).
45. B. L. Osborn, L. Sekut, M. Corcoran, C. Poortman, B. Sturm, G. Chen, D. Mather, H. L. Lin, and T. J. Parry. Albutropin: a growth hormone–albumin fusion with improved pharmacokinetics and pharmacodynamics in rats and monkeys. *Eur. J. Pharmacol.* **456**:149–158 (2002).

doi:10.1016/j.jmb.2006.08.056 J. Mol. Biol. (2006) 363, 702–712

JMB

Available online at www.sciencedirect.com

ScienceDirect

ELSEVIER

Chain Length-dependent Binding of Fatty Acid Anions to Human Serum Albumin Studied by Site-directed Mutagenesis

Ulrich Kragh-Hansen[1]*, Hiroshi Watanabe[2], Keisuke Nakajou[2] Yasunori Iwao[2] and Masaki Otagiri[2]

[1]*Department of Medical Biochemistry, University of Aarhus, Ole Worms Allé Building 1170 DK-8000 Århus C Denmark*

[2]*Department of Biopharmaceutics Graduate School of Pharmaceutical Sciences Kumamoto University 5-1 Oe-honmachi Kumamoto 862-0973 Japan*

**Corresponding author*

Human serum albumin is the most abundant protein in the circulatory system, and one of its principal functions is to transport fatty acids. Binding of octanoate, decanoate, laurate and myristate was studied by a rate-of-dialysis technique. The primary association constants increased, but not linearly, with chain length. The number of high-affinity sites also increased with chain length; octanoate and decanoate bind to one such site, whereas laurate and myristate most probably bind to two sites. Albumin is composed of three homologous helical domains (I–III), which can be subdivided into two subdomains (A and B). For getting information about the positions of the high-affinity sites we produced 13 recombinant isoforms mutated in four different subdomains. Results obtained with these albumins are in accordance with the following model: octanoate and decanoate bind to a single site in subdomain IIIA, laurate binds to sites in subdomains IIIA and IIIB, whereas myristate binds in subdomains IB and IIIB. The results also showed that primary fatty acid binding is sensitive to amino acid substitutions in other parts of the protein. This is in contrast to the effect of amino acid substitutions of genetic albumin variants (alloalbumins). Usually these substitutions, which are situated at the surface of the protein, have no effect on fatty acid binding. Binding of fatty acid anions to different high-affinity sites and the sensitivity of these sites to amino acid substitutions elsewhere in the protein (and perhaps also to other types of modifications) are important factors that could effect simultaneous binding of other ligands, e.g. in patients treated with albumin-binding drugs.

Keywords: human serum albumin; albumin mutants; fatty acid binding; high-affinity sites; conformational changes

Introduction

Human serum albumin (HSA) is a single-chain protein synthesized in and secreted from liver cells. Normally, it is a simple protein, i.e. it is without prosthetic groups and covalently bound carbohydrate or lipid.[1] Based on X-ray crystallographic analyses of HSA and its recombinant version (rHSA), the polypeptide chain of 585 amino acid residues forms a heart-shaped protein with dimensions 80 Å×80 Å×80 Å and with a thickness of 30 Å.[2,3] The protein has about 67% α-helix but no β-sheet and is composed of three homologous domains (I–III). Each of these has two subdomains (A and B) with distinct helical folding patterns that are connected by flexible loops.[2,3]

HSA is one of the principal compounds of the blood, and, due to its high concentration in plasma (ca 0.6 mM), it is responsible for about 80% of the colloid osmotic pressure of that fluid.[1] In addition, albumin has several other functions. For example, it is an important anti-oxidant, possesses enzymatic properties and serves as a transport and depot protein for numerous compounds.[1,4] Under physiological conditions, one of the primary transport roles of HSA is to carry fatty acids, which are poorly soluble in an aqueous environment, and usually the

Abbreviations used: HSA, human serum albumin; rHSA, recombinant HSA; Site I and II, Sudlow's drug binding sites; Site 1–9, fatty acid binding sites.

E-mail address of the corresponding author: ukh@biokemi.au.dk

protein carries 0.3–1 mol of fatty acid per mol of protein,[5] but this value can raise to 6 after maximum exercise or adrenergic stimulation.[1] Here, we have examined the binding of octanoate, decanoate, laurate and myristate to HSA. Although medium-chain fatty acids normally constitute a minor fraction of the non-esterified fatty acids in plasma, interest in the binding of medium-chain fatty acids exists as the level of these can be greatly elevated in certain disease states, in patients fed intravenous medium chain triacylglycerols and in infants treated for low birth weight.[1] Our results showed principal differences in binding of the four fatty acids to HSA.

In an attempt to examine high-affinity fatty acid binding in more detail we also studied their binding to mutants of rHSA. As a guide to select positions for mutagenesis we used the crystal structures of rHSA complexed with fatty acids. Curry and co-workers have studied the structure of rHSA to which, e.g. decanoate, laurate or myristate was bound and observed binding of eight to ten fatty acid molecules per albumin molecule.[6–8] By contrast, the crystal structure of rHSA–octanoate is still unknown. Other types of experiments, many performed with albumin fragments, have suggested that among the eight to ten sites the high-affinity ones are placed in subdomains IB, IIIA and/or IIIB.[1,9] Therefore, we examined high-affinity binding of the four fatty acids mentioned to R117A and H146A (subdomain IB), Y401A, R410A, Y411F, Y411A, Y411S and the double-residue mutant R410A/Y411A (subdomain IIIA) and K525A (subdomain IIIB), all of which were produced using the yeast species *Pichia pastoris* as the expression system.

The unique ligand binding properties of HSA also include binding of a large number of exogenous compounds such as drugs. High-affinity drug binding usually takes place to Sudlow's Site I or Site II.[10] Site I is pre-formed as a pocket within the core of subdomain IIA and involves the lone tryptophan of the protein (Trp214),[2,3,11] whereas the smaller Site II has been assigned to subdomain IIIA and seems to differ from Site I with respect to shape and polarity.[11] In addition to drugs, fatty acid anions can bind to these two sites. Therefore, we also studied high-affinity binding of octanoate, decanoate, laurate and myristate to Site I and Site II mutants, because in this way we could perhaps get some molecular information about the often observed interplay between albumin-bound fatty acids and drugs.[1,4,12] Thus, in addition to studying fatty acid binding to mutations of, e.g., Arg410 and/or Tyr411, which are components of Site II, we also included the Site I mutants K199A, W214A, R218H and H242Q in the present study.

Results and Discussion

Fatty acid binding to HSA

Binding of octanoate, decanoate, laurate and myristate to HSA was investigated by the rate-of-dialysis technique.[13] This approach was used, because it is well suited to quantify high-affinity ligand binding, and because it is less sensitive to any unbound radiochemical impurities in the batches of radioactively labeled fatty acids than, e.g., equilibrium dialysis.[13] The results obtained with the same total concentrations of the fatty acids and a constant protein concentration are given as Scatchard plots in the insets to Figure 1. From the inset to Figure 1(a) it is seen that octanoate binding takes place to one high-affinity site and to a site with much lower affinity. It is probable that binding experiments with still higher octanoate concentrations can reveal the existence of additional low-affinity sites.[14] From the examples given in the main part of Figure 1(a) it is seen in greater detail how K_1 was estimated; the average value of K_1 (±SD) for 14 determinations performed in triplicate is $2.0(\pm0.1)\times10^6$ M^{-1}. The proposal of only one high-affinity site for octanoate is in accordance with previous findings.[15]

As shown in the inset to Figure 1(b), decanoate binds to more sites, i.e. apparently to one site with a high affinity and to some sites with a low affinity. In this case, K_1 was calculated as $5.1(\pm0.2)\times10^6$ M^{-1} ($n=14$). In 1972, Ashbrook *et al.* published a similar study but based on equilibrium dialysis, and also these authors characterized binding by the stepwise equilibrium method (cf. equation (3)).[16] However, the downward progression of their binding curve is less steep than found in our case, and their K_1 was only 1.03×10^5 M^{-1}. The differences between the results of the two studies can be explained by the fact that Ashbrook *et al.* used a high concentration of chloride ions (116 mM NaCl+4.9 mM KCl) in their medium, because chloride ions are known to diminish simultaneous binding of medium-chain fatty acids to HSA.[17]

^{13}C NMR spectroscopic studies have revealed differences in binding between decanoate and other fatty acid anions, all with ^{13}C-enriched carboxyl carbon atoms.[14] Thus, chemical shift data showed that the first molecule of octanoate and decanoate either bind differently to the same site or bind to different sites of HSA. Furthermore, differences were found in binding characteristics for decanoate and laurate.

In contrast to binding of octanoate and decanoate, binding of laurate takes place to more than one high-affinity site (Figure 1(c), inset). Several authors have proposed binding to two high-affinity sites, both on the basis of a Scatchard analysis[18,19] and from a stoichiometric approach.[20] Ashbrook *et al.*, using a high chloride ion concentration in the medium, did not agree with that binding model but suggested that laurate binding is best described by a series of decreasing K-values.[21] However, the proposal of two high-affinity sites has been supported by ^1H NMR spectroscopic studies.[22] Still, a K_1-value can be estimated, cf. main part of Figure 1(c), and for laurate it was found to be $3.4(\pm0.2)\times10^7$ M^{-1} ($n=14$). This value is comparable to, or slightly higher than, those previously published.[20,23,24]

K_1 for myristate binding was determined to be $3.6(\pm0.3)\times10^7$ M^{-1} ($n=14$), a value which is similar